LAPLACIANS ON A FAMILY OF QUADRATIC JULIA SETS I

TARYN C. FLOCK AND ROBERT S. STRICHARTZ

ABSTRACT. We describe families of Laplacians on Julia Sets $\mathcal{J}_c$ for quadratic polynomials $P(z) = z^2 + c$ in the spirit of Kigami's construction of Laplacians on p.c.f. self-similar fractals. We consider an infinite family of Julia sets for c in the interior of a bulb in the Mandelbrot set that includes the basilica and the Douady rabbit. We use the external ray parametrization of the Julia set which represents the Julia set as a circle with some points identified. There is a one-dimensional space of P-invariant energies that arises from the standard energy on the circle, but we show surprisingly that there are higher dimensional spaces of energies invariant under iterates of P. There are two natural measures associated with the dynamics of P on $\mathcal{J}$, the equilibrium measure μ, which is P-invariant but ignores the geometric aspects of the P action, and the conformal measure ν, which is not P-invariant but does transform according to a power of the Jacobian of the mapping. The P-invariant Laplacian Δ_μ is built from the P-invariant energy and the measure μ. This Laplacian will depend only on the topological type of $\mathcal{J}$ (so for quasicircles, it just gives the usual Laplacian on the circle). The conformal Laplacian Δ_ν is built from the P-invariant energy and the measure ν.

We describe numerical procedures to approximate the eigenvalues and eigenfunctions of the Laplacians Δ_μ and Δ_ν and present the computational results. For Δ_μ we identify a 4-element ($\mathbf{Z}_2 \oplus \mathbf{Z}_2$) group of symmetries. In the case of the basilica the symmetries are generated by horizontal and vertical reflections, but in the case of the rabbit and other Julia sets the symmetries are more hidden (only $z \to -z$ is obvious). Based on these symmetries we are able to classify eigenfunctions and explain the computational data.

1. INTRODUCTION

Analysis on fractals has been widely developed (see [Bar98], [Kig01], [Str06] and the references therein for a sample). The approach pioneered by Kigami has at its core a Laplacian that is built from energy and measure. Most of the examples studied so far have been linear fractals, such as the Sierpinski gasket, Sierpinski carpet, and Vicsek set. Recently [RT09] extended Kigami's approach to the basilica Julia sets. The Julia set $\mathcal{J}_c$ for the quadratic polynomials $P(z) = z^2 + c$ with c in the Mandelbrot set is a well studied class of nonlinear fractals that are both

connected and finitely ramified (they may be disconnected by removing a finite number of points) and so fit nicely into the Kigami paradigm:

(i) Approximate the fractal by a sequence of graphs Γ_m with vertices V_m and edge relation $x \underset{m}{\sim} y$. We want the vertices to be nested,

$$(1.1) \qquad\qquad\qquad V_0 \subseteq V_1 \subseteq V_2 \subseteq \dots$$

with the union

$$(1.2) \qquad\qquad\qquad V_* = \bigcup_{m=0}^{\infty} V_m,$$

a dense subset of the fractal.

(ii) On each graph Γ_m construct an energy

$$(1.3) \qquad \mathcal{E}_m(u, v) = \sum_{x \underset{m}{\sim} y} c_m(x, y)(u(x) - u(y))(v(x) - v(y)).$$

The conductances $c_m(x, y)$ are positive and may be interpreted as reciprocals of resistances, where the graph is viewed as an electric network with resistors of resistance $1/c_m(x, y)$ connecting the nodes x, y. For any function u defined on V_m, its *harmonic extension* $\tilde{u}$ to V_{m+1} is defined to be the extension that minimizes energy:

$$(1.4) \qquad\qquad\qquad \mathcal{E}_{m+1}(\tilde{u}, \tilde{u}) \leq \mathcal{E}_{m+1}(u, u),$$

where $\tilde{u}$ restricted to V_m equals u. We want to have the identity

$$(1.5) \qquad\qquad\qquad \mathcal{E}_{m+1}(\tilde{u}, \tilde{u}) = \mathcal{E}_m(u, u).$$

It follows that for any function u defined on V_* we have increasing energy:

$$(1.6) \qquad\qquad \mathcal{E}_0(u, u) \leq \mathcal{E}_1(u, u) \leq \mathcal{E}_2(u, u) \leq \dots,$$

and so the definition

$$(1.7) \qquad\qquad\qquad \mathcal{E}(u, u) = \lim_{m \to \infty} \mathcal{E}_m(u, u)$$

always makes sense. If we define the domain *dom* $\mathcal{E}$ to be the functions with $\mathcal{E}(u, u) < \infty$, then

$$(1.8) \qquad\qquad\qquad \mathcal{E}(u, v) = \lim_{m \to \infty} \mathcal{E}_m(u, v)$$

is always finite for $u, v \in$ *dom* $\mathcal{E}$.

(iii) We choose a measure μ on the fractal and define a Laplacian Δ_μ by the weak formulation

$$(1.9) \qquad\qquad -\mathcal{E}(u, v) = \int (\Delta_\mu u) v \, d\mu \quad \text{for } v \in \text{dom } \mathcal{E}.$$

There is also a pointwise formula for $\Delta_\mu u$ on V_* as a limit of graph Laplacians

$$(1.10) \qquad\qquad \Delta_\mu u(x) = \lim_{m \to \infty} \frac{1}{\int \psi_x^{(n)}} \Delta_m u(x),$$

where

$$(1.11) \qquad\qquad \Delta_m u(x) = \sum_{y \underset{m}{\sim} x} c_m(x, y)(u(y) - u(x))$$

and $\psi_x^{(m)}$ is the harmonic extension of the function $y \to \delta_{xy}$ on V_m.

In the context of p.c.f. self-similar fractals, the energy is taken to have a self-similar structure. In the context of Julia sets we want to relate the energy to the dynamics of the action of P on $\mathcal{J}$. The simplest requirement is P-invariance:

$$
(1.12) \qquad \mathcal{E}(u \circ P, v \circ P) = c_1 \mathcal{E}(u, v)
$$

(implicit in this is the statement that $u \in dom\ \mathcal{E}$ implies $u \circ P \in dom\ \mathcal{E}$). A somewhat weaker requirement is

$$
(1.13) \qquad \mathcal{E}(u \circ P^{(k)}, v \circ P^{(k)}) = c_k \mathcal{E}(u, v)
$$

for some fixed k. Obviously (1.12) implies (1.13) for all k. In the case of the unit circle ($c = 0$), all solutions of (1.13) are multiples of the standard energy

$$
(1.14) \qquad \mathcal{E}(u, v) = \int_0^{2\pi} u'(\theta) v'(\theta) d\theta,
$$

and so (1.13) implies (1.12). We will see in section 3 that in general there are more solutions to (1.13) than to (1.12).

We use the method of external rays developed by Doaudy and Hubbard [DH84] to parameterize the Julia set. Consider the Riemann mapping from the exterior of the unit circle to the exterior of $\mathcal{J}$ (normalized so that ∞ is mapped to ∞ and the point $z = 1$ is mapped to the repelling fixed point of P). We denote by ϕ the restriction of the continuous extension of this mapping to the unit circle C (this exists for c in a hyperbolic component of the Mandlebrot set). For simplicity we parametrize the circle by $x = \frac{\theta}{2\pi}$ in $[0, 1]$. For the Julia sets we work with, ϕ is a continuous mapping onto $\mathcal{J}$, but typically it is not one-to-one (only in the case of quasicircles is it one-to-one). Thus $\mathcal{J}$ is realized as a quotient of C by an infinite set of identifications of points. In section 2 we describe these identifications explicitly and give diagrams illustrating them. Since ϕ intertwines the action P on $\mathcal{J}$ and $z \rightarrow z^2$ on C, the dynamics of P are easily read from this parametrization. We also easily obtain a sequence of graphs Γ_m on $\mathcal{J}$ (obtained after identifying points on graphs Γ'_m on C), where the vertices in V_{m+1} are obtained from V_m by applying P^{-1}.

As noted we require that c is in a hyperbolic component of the Mandelbrot set. Equivalently we require that P_c has an attracting fixed cycle. This cycle will be unique, so we may classify the Julia sets we work with by the period of this cycle, k. Note that k will be constant on each hyperbolic component. The second requirement demands some notation. Call the connected component of c in the filled in Julia set U_1. This is the region labeled 1 in Figure 1.1. We then require that the root point of U_1 be a fixed point of P. This implies the root has period k. Our last requirement is that the combinatorial rotation number of c be ± 1, i.e. that $P(U_1)$ is the next domain in the filled in Julia set connected to the root in the clockwise or counterclockwise direction. In the diagram below, this means we require that either $P(U_1) = U_2$ or $P(U_2) = U_1$. Given these restrictions, we take c in the main cardioid ($k = 1$) or in a series of bulbs directly adjoining it, namely the $\frac{\pm 1}{k}$-bulbs. See [Bra89] for further details.

In section 3 we study the energies $\mathcal{E}_m$ on the graphs Γ_m that are naturally obtained from energies $\mathcal{E}'_m$ on the graphs Γ'_m on C. The lengths of the intervals on C between consecutive vertices are not all equal, but follow a pattern $\delta_m, 2\delta_m, 4\delta_m, ..., 2^{k-1}\delta_m$, where k depends on the Julia set ($k = 1$ for the circle,
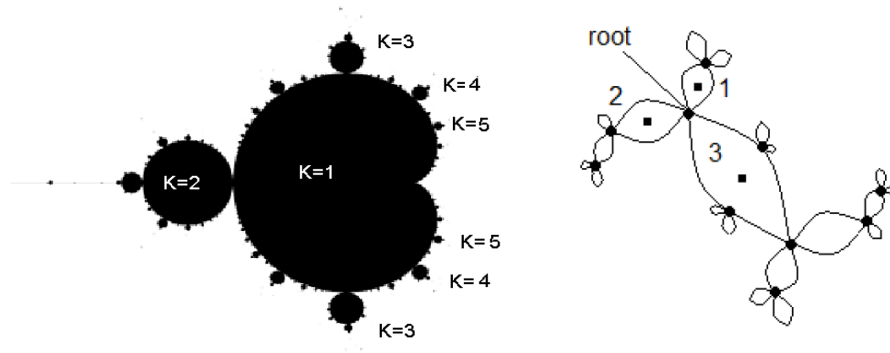
FIGURE 1.1. **Left:** Mandelbrot with the bulbs that satisfy our criterion marked by their k value. **Right:** The rabbit with the root and the attracting cycle $(0,c,c^2 + c)$ marked. The numbers reflect the dynamics of P (region 1 maps to region 2 maps to region 3).

$k = 2$ for the basilica, and $k = 3$ for the rabbit) and $\delta_m = 2^{-m}\delta$. For the standard energy on C, resistances are proportional to length, so on Γ'_m

$$(1.15) \quad E'_m(u,v) = c \sum_m \sum_{j=0}^{k-1} 2^{m-j}(u(x_{nk+j+1}) - u(x_{nk+j}))(v(x_{nk+j+1}) - v(x_{nk+j})).$$

After identifying points (the vertices in V'_m have the property that all points identified with a vertex in V'_m are also in V'_m) and multiplying by the renormalization factor $2^{\frac{1-k}{k}m}$, we obtain our energy $\mathcal{E}_m$ on Γ_m. However, it turns out that (1.5) does not hold (if $k \geq 2$). Instead we have

$$(1.16) \quad \mathcal{E}_{m+k}(\tilde{u}, \tilde{u}) = \mathcal{E}_m(u, u),$$

where $\tilde{u}$ is the harmonic extension to V_{m+k}.

Thus we obtain k different energies

$$(1.17) \quad \mathcal{E}^{(j)}(u,v) = \lim_{m \to \infty} \mathcal{E}_{km+j}(u,v) \text{ for } j = 0, 1, ..., k-1.$$

It turns out that each of these energies is invariant under $P^{(k)}$ ((1.13) holds), but

$$(1.18) \quad \mathcal{E}^{(j)}(u \circ P, v \circ P) = 2^{\frac{k+1}{k}} \mathcal{E}^{(j-1)}(u, v).$$

By taking the average

$$(1.19) \quad \mathcal{E}(u,v) = \frac{1}{k} \sum_{j=0}^{k-1} \mathcal{E}^{(j)}(u,v)$$

we obtain a P-invariant energy.

In section 4 we discuss the equilibrium measure μ and conformal measure ν on $\mathcal{J}$, and the Laplacians Δ_μ and Δ_ν constructed from the P-invariant energy (1.18) via (1.9) or (1.10). The measure μ is just the pullback to $\mathcal{J}$ of the normalized

Lebesgue measure on the circle approximated on V_m by the discrete measure that gives equal weight to all vertices and satisfies the P-invariance condition

$$(1.20) \qquad \int_{\mathcal{J}} f \circ P d\mu = \int_{\mathcal{J}} f d\mu.$$

It follows that the Laplacian Δ_μ also satisfies a P-invariance condition

$$(1.21) \qquad \Delta_\mu(u \circ P) = 2^{1+\frac{1}{k}} (\Delta_\mu u) \circ P.$$

In particular, if u is a λ-eigenfunction,

$$(1.22) \qquad -\Delta_\mu u = \lambda u,$$

then $u \circ P$ is a $2^{\frac{1+k}{k}} \lambda$-eigenfunction. In other words, the spectrum of Δ_μ is preserved under multiplication by $2^{1+1/k}$.

Although the invariance condition (1.20) is very simple, it fails to take into account the geometry of the mapping P. The corresponding formula for Lebesgue measure in $\mathbf{R}^n$ would have a Jacobian factor. Since the mapping P is conformal, the Jacobian is a power of $|P'(z)|$. The conformal measure ν is characterized by the condition

$$(1.23) \qquad \int_{\mathcal{J}} f \circ P |P'|^d d\nu = \int_{\mathcal{J}} f d\nu$$

for a constant d that may be identified as the Hausdorff dimension of $\mathcal{J}$. The Laplacian Δ_ν depends on the geometry of $\mathcal{J}$, whereas Δ_μ is the same for all Julia sets with the same topology. If we use the energies $\mathcal{E}^{(j)}$ instead of $\mathcal{E}$ we obtain Laplacians $\Delta_\mu^{(j)}$ and $\Delta_\nu^{(j)}$. We will show that the Laplacians $\Delta_\mu^{(j)}$ all commute, so they have the same eigenfunctions (with different eigenvalues).

In section 5 we discuss the symmetries of Δ_μ. Of course every Julia set has the symmetry $z \to -z$, and this is a symmetry of all the Laplacians. The circle has complete rotation symmetry. If we look at the basilica ($c = -1$) we see that it is symmetric with respect to the vertical R_V and the horizontal R_H reflections. In the external ray parameterization these are also vertical and horizontal reflections, or $x \to -x$ and $x \to \frac{1}{2} - x$ (the product is $x \to \frac{1}{2} + x$, which corresponds to $z \to -z$). It is clear that these symmetries preserve all the energies and the measure μ, but not the measure ν. So Δ_μ has a $\mathbf{Z}_2 \oplus \mathbf{Z}_2$ symmetry group, and we can subdivide the eigenfunctions into four types according to even and odd behavior under R_V and R_H. We write these as $++, +-, -+,$ and $--$. It is easy to see that an eigenfunction u has the form $u = u' \circ P$ for another eigenfunction u' if and only if it has the type $++$ or $--$. We call such an eigenfunction *derived*, and all others *primitive*. We show that reflectional symmetries of Δ_μ exist on all the Julia sets we study. We continue to denote them by R_V and R_H, although they are not simple vertical and horizontal reflections on the ambient plane and do not have the same description in the external ray parameterization.

In section 6 we describe the algorithms we use to compute approximation to the conformal measure ν, the eigenfunctions, and eigenvalues of Laplacians. We present numerical data in graphical form for a few examples of quasicircles, the basilica, and the rabbit. Further computational results may be found in [Flo08]. We also show the eigenvalue counting functions and Weyl ratios. We have numerical evidence for eigenvalue gaps and spectral clusters.

In section 7 we discuss the properties of the eigenfunctions of Δ_μ that are visible in the data, using the symmetries of Δ_μ. In particular, we can predict the multiplicities of eigenspaces and the supports of eigenfunctions. This already goes beyond the results for the basilica obtained in [RT09].

Each Julia set can be viewed as the closure of a countable collection of topological circles that intersect at junction points (the junction points are dense in each circle) where exactly k circles meet. In [RT09] this structure is used to describe the energy. In section 8 we consider the restrictions of the eigenfunctions to one of these circles that we call the *central circle*. It corresponds to a Cantor set in the external ray parameterization. The portions of $\mathcal{J}$ that correspond to the complementary intervals of this Cantor set we will call *loops*. We will show that generically the restriction to a loop of any eigenfunction is determined by the eigenvalue, the size of the loop, and the value at the junction point. We will use this to produce an eigenfunction equation for a different Laplacian on the central circle.

Further development of the methods of this paper may be found in [ADS10]. In particular, it treats a wider class of Julia sets, provides an alternate construction of the energy for our examples, and considers covering spaces and blowups of Julia sets.

2. EXTERNAL RAY PARAMETERIZATION

We start our graph approximation from a fixed point z_0 of P lying in $\mathcal{J}$. For such a point we have $z^2 + c = z$, which can be solved using the quadratic formula to produce $z_\pm = \frac{1 \pm \sqrt{1-4c}}{2}$. z_+ will be a repelling fixed point (and thus in the Julia set) for all values of c. The same will be true of z_- for c outside the main cardioid of the Mandlebrot set ($k \geq 2$). We take $z_+ = z_0$ when $k = 1$ and $z_- = z_0$ otherwise. As this point is chosen such that $P(z_0) = z_0$, we have that $\phi(P(z_0)) = \phi(z_0)$ and thus that $2x_0 (mod 1) = x_0$, where $x_0 = \phi(z_0)$. Given this we take $V_0' = \{x : x = \phi(z_0)\}$, namely

$$(2.1) \qquad\qquad V_0' = \left\{ \frac{2^j}{2^k - 1} \right\}, \quad j = 0, 1, \ldots, k - 1.$$

These points divide the circle into k intervals

$$(2.2) \qquad\qquad \left[\frac{2^j}{2^k - 1}, \frac{2^{j+1}}{2^k - 1} \right]$$

of lengths $\frac{2^j}{2^k-1}$ in the counterclockwise order. These points are all identified to give a single point in V_0.

We then define V_1' by $2V_1' = V_0$ (double cover). In other words, the points in V_1' have the form $\frac{1}{2}x$ and $\frac{1}{2}x + \frac{1}{2}$ as x varies over V_0'. Note that $V_0' \subset V_1'$. This is obvious for $\frac{2^j}{2^k-1}$ with $j \leq k-2$, but $\frac{2^{k-1}}{2^k-1}\frac{1}{2} = \left(\frac{1}{2^k-1} \right) + \frac{1}{2}$. The remaining k points in $V_1' \backslash V_0'$ are $\frac{1}{2}\left(\frac{2^j}{2^k-1} \right) + \frac{1}{2}$ for $j = 1, \ldots, k-1$ and $\frac{1}{2}\left(\frac{1}{2^k-1} \right)$. Note that they all lie in the interval $\left[\frac{2^{k-1}}{2^k-1}, \frac{1}{2^k-1} \right]$. The points in V_1' divide the circle into two cycles of intervals of length $\frac{1}{2}\frac{2^j}{2^k-1}$ for $j = 0, 1, ..., k-1$ in counterclockwise order. An equivalent description of the passage from V_0' to V_1' is the following: leave all the short intervals (of length $\frac{2^j}{2^k-1}$ for $j \leq k-2$) alone and subdivide the long intervals (of length $\frac{2^{k-1}}{2^k-1}$) into short intervals of lengths $\frac{2^j}{2^k-1}$ for $j \leq k-2$ and two of length

$\frac{1}{2}\frac{1}{2^k-1}$. In passing from V_1' to V_1 we maintain the identification of points in V_0 and identify the k new points in the long intervals. If we make V_1' into a graph Γ_1' by joining adjacent points on the circle by edges, then the induced graph Γ_1 has two edges joining its two vertices and two sets of $k-1$ self-edges at each point. These self-edges do not contribute to the energy, and so we will ignore them. The cases $k=2$ and $k=3$ are illustrated in Figure 2.1.
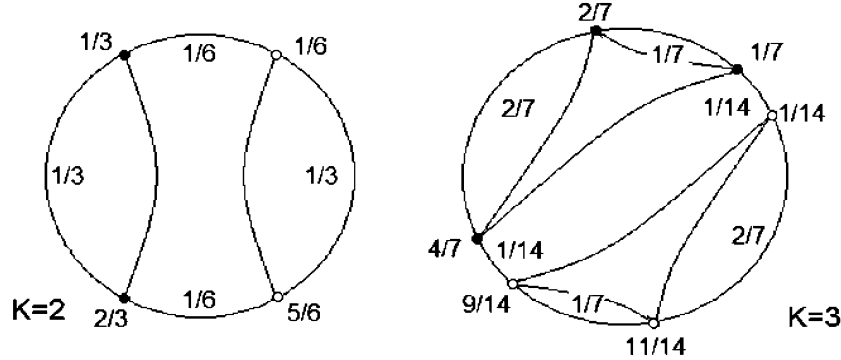

FIGURE 2.1. The vertices in V_0 in dark dots and in $V_1\backslash V_0$ in open dots. The lengths of the intervals are marked.

We can describe in similar terms the passage from V_m' to V_{m+1}'. There are $2^m k$ points in V_m' that are identified to 2^m points in V_m. The points V_m' subdivide the circle into 2^m cycles of intervals of lengths $\frac{1}{2^m}\frac{2^j}{2^k-1}$ for $j=0,...,k-1$ in counterclockwise order. The new points in $V_{m+1}'\backslash V_m'$ lie in the long intervals of length $\frac{1}{2^m}\frac{2^{k-1}}{2^k-1}$ and subdivide each such interval into short intervals of length $\frac{1}{2^m}\frac{2^j}{2^k-1}$ for $j=0,...,k-1$ and two intervals of length $\frac{1}{2^{m+1}}\frac{1}{2^k-1}$ at the ends (note that $\sum_{j=0}^{k-2}\frac{1}{2^m}\frac{2^j}{2^k-1}+2\frac{1}{2^{m+1}}\frac{1}{2^k-1}=\frac{1}{2^m}\frac{2^{k-1}}{2^k-1}$). The k points in each long interval are identified when we pass from V_{m+1}' to V_{m+1}. Figure 2.2 shows several stages of subdivision for $k=2$ and Figure 2.3 does the same for $k=3$.
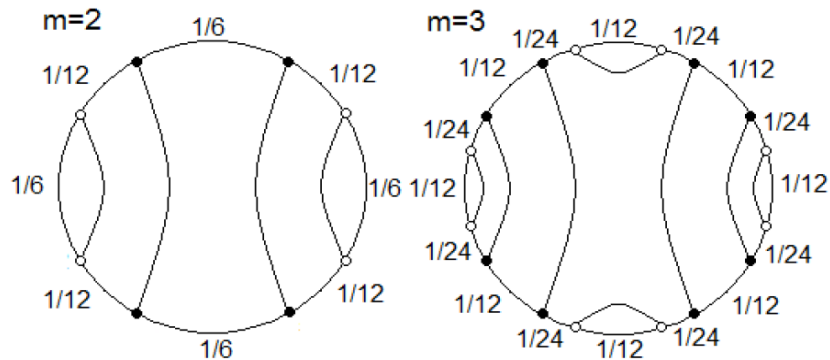

FIGURE 2.2. $k=2$. The vertices in $V_m\setminus V_{m-1}$ are labeled with open dots, and the lengths of the intervals are marked.
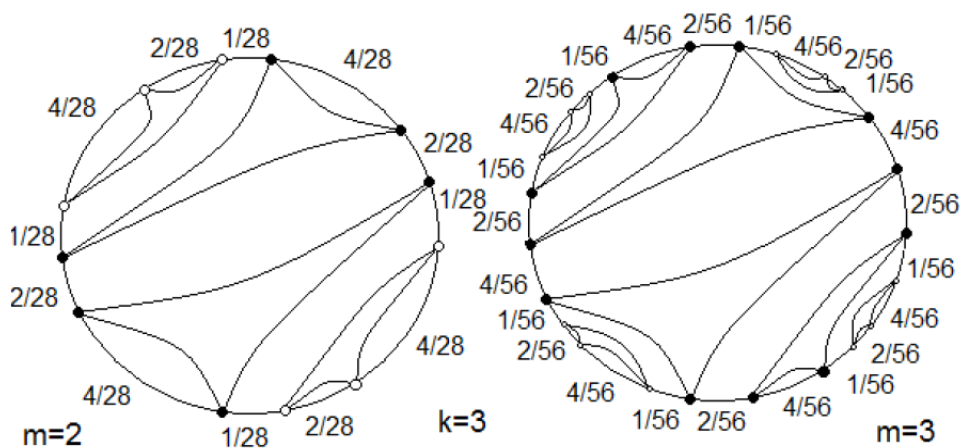
FIGURE 2.3

Next we describe the mapping ϕ from the circle to the Julia set in terms of the points in V_m. The point in V_0 is mapped to the fixed point of P that is a junction point on the central circle. Then, inductively, the points in V_{m+1} are mapped to the preimages of the points in V_m under P. This is illustrated for the basilica ($k = 2$) and the rabbit ($k = 3$) in Figures 2.4 and 2.5. Note that the intervals in V_1' get mapped as follows: in each half the $k - 1$ longest intervals that correspond to the self-edges get mapped to $k - 1$ loops that join the central circle at either end, while the two short intervals get mapped to the central circle together with all the other loops that join it. These loops are images of intervals inside the short intervals, so the central circle is the image of their complement, a set of measure zero of Cantor type (it is not strictly speaking a Cantor set because it contains isolated points).
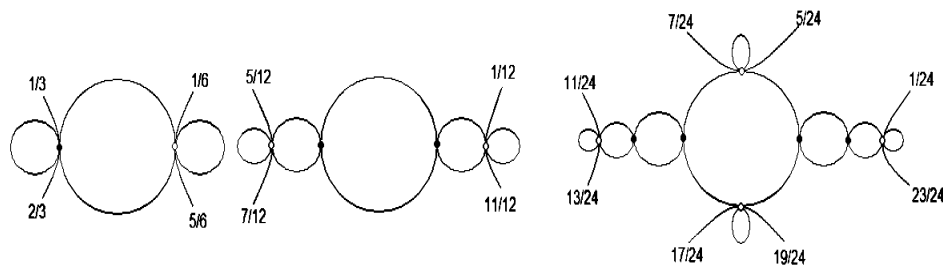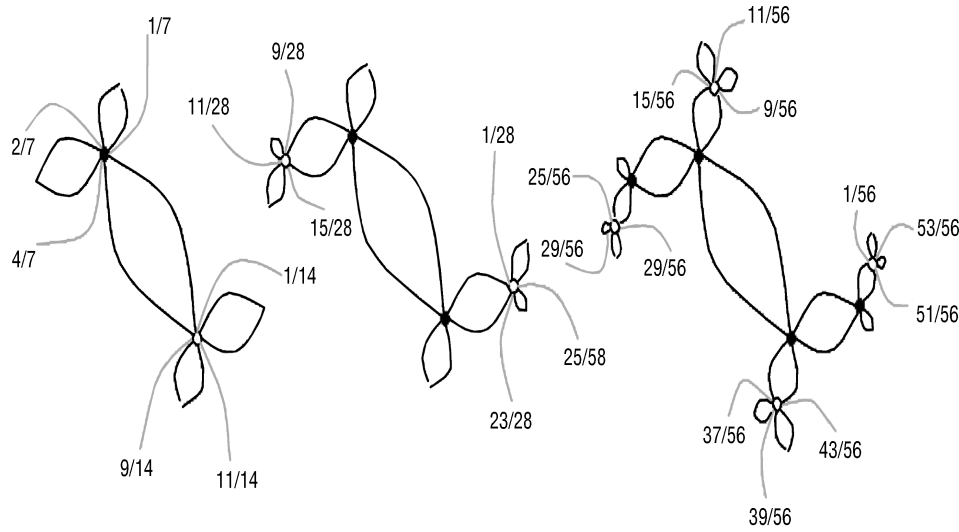

FIGURE 2.4

1/7
9/28
11/28
2/7
4/7
11/56
15/56
9/56
1/28
25/56
15/28
1/14
29/56
29/56
1/56
53/56
51/56
25/58
23/28
37/56
43/56
9/14
11/14
39/56

FIGURE 2.5

3. ENERGIES

The first step is to define energies E_m on the graphs Γ_m. Consider the natural energy E'_m on Γ'_m defined by

$$(3.1) \qquad E'_m(u,v) = \sum_{x' \underset{m}{\sim} y'} \frac{1}{|x'-y'|}(u(x')-u(y'))(v(x')-v(y')) \quad (x',y' \in V'_m).$$

In other words, we take a resistance $|x'-y'|$ equal to the length of the interval connecting the consecutive vertices x', y'. If u and v are defined on V_m, then we can regard them also as functions on V'_m which take the same value on identified points. Thus it makes sense to define

$$(3.2) \qquad\qquad\qquad E_m(u,v) = E'_m(u,v).$$

In terms of the graph Γ_m, each vertex x has $2k$ edges of lengths $\frac{1}{2^m}\frac{2^j}{2^k-1}$ for $j = 0,1,\ldots,k-1$, each length repeated twice. Some of the edges may be self-edges, and some of the neighbors may repeat twice. Thus $E_m(u,v)$ has the form

$$(3.3) \qquad E_m(u,v) = \sum_{x \underset{m}{\sim} y} c_m(x,y)(u(x)-u(y))(v(x)-v(y)) \quad (x,y \in V_m),$$

where the conductance $c_m(x,y)$ is the sum of $\frac{1}{|x'-y'|}$ for all pairs (x',y') mapping to (x,y) with x',y' consecutive vertices in V'_m.

The action of P on $\mathcal{J}$ intertwines the action $x \to 2x$ on C, so we will continue to write $P(x) = 2x$. We want to compute $E_m(u \circ P, v \circ P) = E'_m(u \circ P, v \circ P)$. The action of P maps V_m to V_{m-1} in a two-to-one fashion and respects the identification of points. We have $E'_m(u \circ P, v \circ P) = 2^2 E'_{m-1}(u,v)$, one factor of 2 coming from the double covering and one factor of 2 arising from the doubling of the length of intervals under P. Thus

$$(3.4) \qquad\qquad\qquad E_m(u \circ P, v \circ P) = 4E_{m-1}(u,v).$$

We will also need the iterated version

$$(3.5) \qquad E_m(u \circ P^{(k)}) = 4^k E_{m-k}(u, v).$$

Now suppose u is defined on V_m, and we want to compute the harmonic extension $\tilde{u}$ to V_{m+1}. Each new point x in $V_{m+1} \backslash V_m$ consists of k identified points in a long interval of length $\frac{1}{2^m} \frac{2^{k-1}}{2^k-1}$ between points y' and z' in V_m'. The contribution to $E_{m+1}(\tilde{u}, \tilde{u})$ involving $\tilde{u}(x)$ is then

$$(3.6) \qquad 2^{m+1}(2^k - 1) \left((\tilde{u}(x) - u(y'))^2 + (\tilde{u}(x) - u(z'))^2 \right).$$

This is clearly minimized by setting

$$(3.7) \qquad \tilde{u}(x) = \frac{1}{2}(u(y') + u(z')),$$

which makes (3.6) equal to

$$(3.8) \qquad 2^m(2^k - 1)(u(y') - u(z'))^2.$$

If y' and z' are identified in V_m, this is just 0. Otherwise, it replaces the contribution

$$(3.9) \qquad 2^{m-k+1}(2^k - 1)(u(y') - u(z'))^2$$

to $E_m'(u, u)$ associated to the adjacent points $y', z' \in V_m'$. Note that (3.8) is simply (3.9) multiplied by 2^{k-1}. On the other hand, for adjacent points y', z' in V_m' that are separated by a short interval of length $\frac{1}{2^m} \frac{2^j}{2^k-1}$ for $j \leq k - 2$, the contribution to E_{m+1}' is the same as for E_m'. Thus we definitely do not have $E_{m+1}(\tilde{u}, \tilde{u})$ equal to a constant multiple of $E_m(u, u)$.

Lemma 3.1. *For the harmonic extension $\tilde{u}$ of u from V_m to V_{m+k}, we have*

$$(3.10) \qquad E_{m+k}(\tilde{u}, \tilde{u}) = 2^{k-1} E_m(u, u).$$

Proof. Consider any pair of adjacent points y', z' separated by an interval of length $\frac{1}{2^m} \frac{2^j}{2^k-1}$. There will be no new points added between them until the passage from $E_{m+k-j-1}$ to E_{m+k-j}. At that stage, the contribution associated to the interval will be multiplied by 2^{k-1}. After that stage, points will be inserted between identified points, so the harmonic extension will be constant and contribute 0 to the energy. Thus every term in the expression (3.1) for $E_m'(u, u)$ gets multiplied by 2^{k-1} yielding (3.10). $\qquad \square$

We thus make the definition

$$(3.11) \qquad \mathcal{E}_m(u, v) = 2^{\left(\frac{1-k}{k}\right)m} E_m(u, v)$$

in order to replace (3.10) with

$$(3.12) \qquad \mathcal{E}_{m+k}(\tilde{u}, \tilde{u}) = \mathcal{E}(u, u).$$

For each $j = 0, 1, \ldots, k - 1$ we have (for u defined on V_k)

$$(3.13) \qquad \mathcal{E}_{j+km}(u, u) \leq \mathcal{E}_{j+k(m+1)}(u, u),$$

and so it makes sense to define

$$(3.14) \qquad \mathcal{E}^{(j)}(u, v) = \lim_{m \to \infty} \mathcal{E}_{j+km}(u, v)$$

on *dom* $\mathcal{E}^{(j)}$ defined to be the set of functions u for which $\mathcal{E}^{(j)}(u, u) < \infty$. In fact the above argument shows that

$$(3.15) \qquad E_m(u, u) < E_{m+1}(\tilde{u}, \tilde{u}) \leq 2^{k-1} E_m(u, u),$$

and so

$$(3.16) \qquad \mathcal{E}_m(u,u) \leq 2^{\frac{k-1}{k}} \mathcal{E}_{m+1}(u,u) \leq 2^{k-1} \mathcal{E}_{m+k}(u,u).$$

This implies

$$(3.17) \qquad 2^{-\frac{(k-1)^2}{k}} \mathcal{E}^{(j+1)}(u,u) \leq \mathcal{E}^{(j)}(u,u) \leq 2^{\frac{k-1}{k}} \mathcal{E}^{(j+1)}(u,u),$$

so $dom\ \mathcal{E}^{(j)}$ is independent of j. Thus we denote it by $dom\ \mathcal{E}$. Note that since the constant in (3.11) is less than one, nonconstant functions in $dom\ \mathcal{E}$ will have $E'_m(u,u)$ going to infinity, and so will have infinite energy when viewed as functions on the circle.

Theorem 3.2. *A function in dom $\mathcal{E}$, when considered as a function on C, is Hölder continuous of order $\frac{1}{2k}$, and*

$$(3.18) \qquad |u(x') - u(y')| \leq c\mathcal{E}^{(j)}(u,u)^{\frac{1}{2}} |x' - y'|^{\frac{1}{2k}} \quad (for\ any\ \ j).$$

Proof. It suffices to show that (3.18) holds when x', y' are adjacent points in V'_m for some m. In that case $|x' - y'|$ is comparable to 2^{-m}. From the definition (3.1) we have

$$(3.19) \qquad |u(x') - u(y')|^2 \leq |x' - y'| E'_m(u,u).$$

From the definition (3.11) we have

$$(3.20) \qquad E'_m(u,u) = 2^{(1-\frac{1}{k})m} \mathcal{E}_m(u,u) \leq c|x' - y'|^{\frac{1}{k}-1} \mathcal{E}_m(u,u).$$

Combining (3.19) and (3.20) we obtain

$$(3.21) \qquad |u(x') - u(y')|^2 \leq c|x' - y'|^{\frac{1}{k}} \mathcal{E}_m(u,u),$$

which easily yields (3.18). $\qquad\square$

It follows that $dom\ \mathcal{E}$ embeds naturally in the continuous functions on $\mathcal{J}$, and $dom\ \mathcal{E}$ modulo constants are a Hilbert space with inner product $\mathcal{E}^{(j)}$ for any j.

By combining (3.4) with the definition (3.11) we obtain

$$(3.22) \qquad \mathcal{E}_m(u \circ P, v \circ P) = 2^{1+\frac{1}{k}} \mathcal{E}_{m-1}(u,v).$$

Theorem 3.3. *If $u \in dom\ \mathcal{E}$, then $u \circ P \in dom\ \mathcal{E}$ and*

$$(3.23) \qquad \mathcal{E}^{(j)}(u \circ P, v \circ P) = 2^{1+\frac{1}{k}} \mathcal{E}^{(j-1)}(u,v).$$

It follows that

$$(3.24) \qquad \mathcal{E}^{(j)}(u \circ P^{(k)}, v \circ P^{(k)}) = 2^{k+1} \mathcal{E}^{(j)}(u,v)$$

so that there is a k-dimensional space of energies satisfying the invariance condition (3.24) under $P^{(k)}$. Moreover, if we define

$$(3.25) \qquad \mathcal{E}(u,v) = \frac{1}{k} \sum_{j=0}^{k-1} \mathcal{E}^{(j)}(u,v),$$

then $\mathcal{E}$ satisfies the P-invariance condition

$$(3.26) \qquad \mathcal{E}(u \circ P, v \circ P) = 2^{1+\frac{1}{k}} \mathcal{E}(u,v).$$

Proof. Replacing m by $j + mk$ in (3.22) and passing to the limit we obtain (3.23). Iterating this k times yields (3.24). It is not difficult to deduce from the discussion preceding Lemma 3.1 that all the energies $\mathcal{E}^{(j)}$ are distinct and linearly independent. Then (3.26) follows from (3.24) and (3.25). $\qquad\square$

4. Laplacians

In order to construct a Laplacian from the energy $\mathcal{E}$, we also need a measure. Since we want the Laplacian to reflect the dynamics of P on $\mathcal{J}$, there are two natural choices. The simplest is the *equilibrium measure* μ, which is just the pullback under $\phi : C \to \mathcal{J}$ of the normalized Lebesgue measure on C,

$$(4.1) \qquad \int_{\mathcal{J}} f d\mu = \int_C f \circ \phi \, dx.$$

For each interval $[a, b]$ in C, the image of $\phi([a, b])$ in $\mathcal{J}$ is assigned measure $b - a$. Since

$$(4.2) \qquad \int_{\mathcal{C}} f(2x) dx = \int_C f(x) dx$$

it follows that μ satisfies the P-invariance condition

$$(4.3) \qquad \int_{\mathcal{J}} f \circ P d\mu = \int_{\mathcal{J}} f d\mu.$$

It is not difficult to see that (4.3) uniquely determines μ up to a constant multiple. Under any local one-to-one inverse of P, the measure is reduced by a factor of $\frac{1}{2}$.

It is easy to approximate μ by the discrete measure on V'_m that assigns equal weight $\frac{1}{2^m k}$ to each point so that on V_m each point has weight 2^{-m}. At first it appears that we could do a better job on V_m by assigning weight to a point x proportional to the length of the two intervals on either side of x, but in fact that would make no difference on V'_m since every point corresponds to k points in V_m with one representative of each weight.

If we look at a picture of $\mathcal{J}$ we see that μ assigns equal measure to loops that appear vastly different in size. If we want a measure that more accurately reflects the geometry of $\mathcal{J}$ in the Euclidean plane, we can use the *conformal measure* ν characterized by the identity

$$(4.4) \qquad \int_{\mathcal{J}} (f \circ P)|P'|^d d\nu = \int_{\mathcal{J}} f d\nu,$$

where d is the unique constant for which there exists a probability measure solution. It is known that d is equal to the Hausdorff dimension of $\mathcal{J}$. Suppose $P : B \to A$ is one-to-one and B is small enough that P' is approximately constant. Then by taking f to be the characteristic function of A, (4.4) tells us that $\nu(A) \approx |P'_{|B}|^d \nu(B)$. So when $|P'|$ is larger the mapping P multiplies the ν measure by a larger factor, and where it is smaller the factor is smaller. Since $|P'(z)| = 2|z|$ in all cases, the enlargement factor just depends on the distance to the origin. In fact, for z inside the circle $|z| = \frac{1}{2}$, the measure is decreased.

To approximate ν by a discrete measure on V_m, we just have to assign weights $w_m(x)$ to all points $x \in V'_m$. To have a probability measure we need

$$(4.5) \qquad \sum_{x \in V'_m} w_m(x) = 1.$$

To approximate (4.4) we want

$$(4.6) \qquad w_m(x) \approx |2\phi(x)|^d w_{m-1}(2x).$$

We can start with $w_0(x) = c$ for the points in V_0' that are identified with the unique point in V_0, and then use (4.6) to inductively define w_m on V_m (in terms of the parameter d). For large values of d

$$(4.7) \qquad \sum_{x \in V_m'} w_m(x)$$

will tend to 0, and for small values of d it will tend to ∞ as $m \to \infty$. The unique value d is the one that lies in between, for which (4.7) remains bounded and has finite limit, and by adjusting the constant c we can make the limit 1. This gives us a slow trial and error algorithm to approximate both the dimension d and the measure ν.

Using the energy $\mathcal{E}$ and these measures, we construct the *equilibrium Laplacian* Δ_μ and the *conformal Laplacian* Δ_ν by (1.9) or (1.10). One could also construct Laplacians $\Delta_\mu^{(j)}$ and $\Delta_\nu^{(j)}$ using the energies $\mathcal{E}^{(j)}$ in place of $\mathcal{E}$.

The equilibrium Laplacian Δ_μ satisfies the P-invariance condition

$$(4.8) \qquad \Delta_\mu(u \circ P) = 2^{1+\frac{1}{k}}(\Delta_\mu u) \circ P$$

as an immediate consequence of (4.3) and (3.26). The following important result is now obvious.

Theorem 4.1. *If u is an eigenfunction of Δ_μ with eigenvalue λ, then $u \circ P^{(n)}$ is also an eigenfunction of Δ_μ with eigenvalue $2^{n(1+\frac{1}{k})}\lambda$. In particular, $2^{(1+\frac{1}{k})}\Sigma_\mu \subseteq \Sigma_\mu$, where Σ_μ denotes the spectrum of Δ_μ.*

Definition 4.2. An eigenfunction u of Δ_μ is called **derived** if there exists u' such that $u = u' \circ P$ or **primitive** if no such u' exists. A derived eigenfunction is of *class D_n* if n is the largest integer such that $u = u' \circ P^{(n)}$ for some eigenfunction u'. A positive eigenvalue $\lambda \in \Sigma_\mu$ is called *derived* or *primitive* according to whether $2^{-(1+\frac{1}{k})}\lambda$ is or is not in Σ_μ, and a derived eigenvalue is of class D_n if n is the largest integer such that $2^{-n(1+\frac{1}{k})}\lambda \in \Sigma_\mu$. *Warning:* the eigenspace of a derived eigenvalue may contain both derived and primitive eigenfunctions.

Theorem 4.3. *An eigenfunction of Δ_μ is derived if and only if it is even under $z \to -z$:*

$$(4.9) \qquad u(-z) = u(z).$$

Conversely, if an eigenfunction of Δ_μ is odd,

$$(4.10) \qquad u(-z) = -u(z),$$

then u is primitive.

Proof. Suppose $u = u' \circ P$ for some eigenfunction u'. Then

$$u(-z) = u'(P(-z)) = u'(P(z)) = u(z)$$

since $P(-z) = P(z)$, so (4.9) holds for derived eigenfunctions. Since (4.10) is incompatible with (4.9), it implies that u is primitive. Finally, suppose (4.9) holds. Define $u'(z) = u(P^{-1}z)$. Note that (4.9) implies that u' is well defined, since both preimages of z under P differ by a minus sign. Then (4.8) shows that u' is an eigenfunction of Δ_μ, so u is derived. $\square$

If an eigenspace has multiplicity 1, then either (4.9) or (4.10) must hold, and this will distinguish the derived and the primitive. However, there are eigenspaces of higher multiplicity, and these split into direct sums of primitive and derived eigenfunctions using the usual even odd splitting of functions (obviously $z \to -z$ commutes with all Laplacians).

The equilibrium Laplacian Δ_μ is defined entirely in terms of identifications on C and the mapping ϕ from C to $\mathcal{J}$, so it is essentially the same for all Julia sets with the same topology. For example, if $\mathcal{J}$ is a quasicircle, then Δ_μ is just the ordinary Laplacian under the parameterization ϕ. From this point of view, the conformal Laplacian is more interesting. However, the price we pay is that we cannot describe the structure of the spectrum of Δ_ν in the same detail as for Δ_μ.

5. Symmetries of the equilibrium Laplacian

The rotation $z \to -z$ is an obvious symmetry of all Julia sets and all our Laplacians. In this section we describe two more symmetries of Δ_μ that we will call *vertical* R_V and *horizontal* R_H reflections. In the case of the basilica ($k = 2$) these are exactly what they are, both on $\mathcal{J}$ and on C. In general they are different, but we will use the same terminology. The basic idea is that on the central circle we will take reflections and at junction points we will permute the loops that join.

First we describe R_H. In Figure 2.1 with $k = 2$ a horizontal reflection maps vertices to vertices, and the same is true in Figure 2.2. However, in Figure 2.1 with $k = 3$, if we reflect about the diameter through $\frac{3}{28}$ and $\frac{17}{28}$, we will permute $\frac{1}{14}$ and $\frac{1}{7}$ and also $\frac{4}{7}$ and $\frac{9}{14}$, but we will not permute $\frac{2}{7}$ and $\frac{11}{14}$. But the intervals $[\frac{1}{7}, \frac{2}{7}]$ and $[\frac{2}{7}, \frac{4}{7}]$ get mapped to two loops that join the central cycle at the same point. Since the order does not matter to the intrinsic geometry of $\mathcal{J}$, we can permute them by replacing $\frac{2}{7}$ by $\frac{3}{7}$, as shown in Figure 5.1.
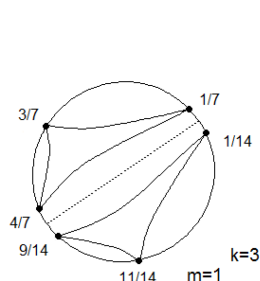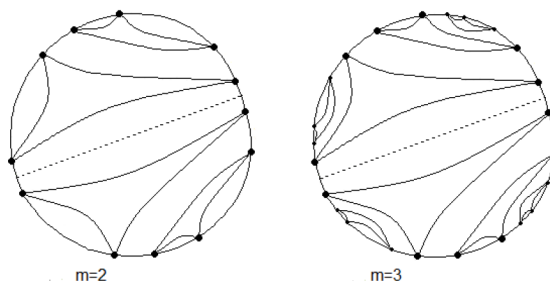
FIGURE 5.1   FIGURE 5.2

Now the reflection permutes all points. Of course we have to continue to permute the order of smaller loops to extend the reflection to the V'_m vertices shown in Figure 2.3 and now seen in Figure 5.2.

The same pattern persists for higher values of m within the loops $[\frac{1}{7}, \frac{4}{7}]$ and $[\frac{9}{14}, \frac{1}{14}]$. These loops are isometric to each other if we do the appropriate permutation of subloops. However, something different has to be done in the interval,

$[\frac{1}{14}, \frac{1}{7}]$ and $[\frac{4}{7}, \frac{9}{14}]$ that map to the central circle and the other loops that join it. At level $m = 4$ we subdivide $[\frac{1}{14}, \frac{1}{7}]$, as shown in Figure 5.3.

FIGURE 5.3

R_H will permute the intervals $[\frac{8}{112}, \frac{9}{112}]$ and $[\frac{15}{112}, \frac{16}{112}]$ (with appropriate subloop swaps as these intervals subdivide for higher values of m), but it will preserve the loops $[\frac{9}{112}, \frac{11}{112}]$ and $[\frac{11}{112}, \frac{15}{112}]$, acting as a reflection on each one in a similar fashion: every time you subdivide a loop into two outer intervals and two inner loops, permute the outer intervals and preserve the inner loops.
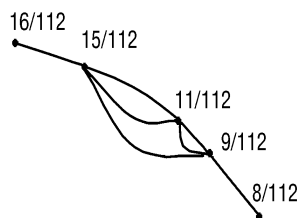
To describe R_V we want a modified reflection about the perpendicular diameter through $\frac{5}{14}$ and $\frac{12}{14}$. This will permute the intervals $[\frac{1}{14}, \frac{1}{7}]$ and $[\frac{4}{7}, \frac{9}{14}]$ with the appropriate swapping of subloops. However, the loops $[\frac{1}{7}, \frac{2}{7}]$, $[\frac{2}{7}, \frac{4}{7}]$, $[\frac{9}{14}, \frac{11}{14}]$ and $[\frac{11}{14}, \frac{15}{14}]$ are all preserved. When they are subdivided the rule is the same as for R_H: the outer two intervals are permuted while the inner two loops are preserved.

It is not hard to see that R_H and R_V commute with Δ_μ, so eigenfunctions may be sorted according to whether they are even or odd. We write the R_V symmetry first, so $+-$ symmetry type means $u \circ R_V = +u$ and $u \circ R_H = -u$, etc. Functions of type $++$ and $--$ satisfy (4.9), and functions of type $+-$ and $-+$ satisfy (4.10). We call the $+-$ type *horizontal* (H) and the $-+$ type *vertical* (V). By Theorem 4.3 we may sort the primitive eigenfunctions into H and V types. The key observation is that we may decompose $\mathcal{J}$ into horizontal (resp. vertical) segments joined at fixed points of R_H (resp. R_V), such that the H eigenfunctions behave independently on the segments: they can be multiplied by a different constant on each segment and remain eigenfunctions. In particular, if the eigenspace has multiplicity one, then the eigenfunction must be supported in one segment.

It is easy to see the segments on the basilica. The fixed points of R_V are the junction points along the horizontal axis. In the C parameter they are $\frac{1}{3} \sim \frac{2}{3}, \frac{1}{6} \sim \frac{5}{6}, \frac{1}{12} \sim \frac{11}{12}, \frac{5}{12} \sim \frac{7}{12}$, ... (in general $\frac{1}{3 \cdot 2^m} \sim 1 - \frac{1}{3 \cdot 2^m}$, $\frac{1}{2} - \frac{1}{3 \cdot 2^m} \sim \frac{1}{2} + \frac{1}{3 \cdot 2^m}$), so the vertical segments are just the intersection of $\mathcal{J}$ with the vertical strips bounded by the vertical lines through the fixed points as shown in Figure 5.4.
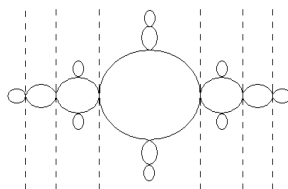

FIGURE 5.4

Similarly, the fixed points of R_H are the junction points along the vertical axis, with C parameters $\frac{5}{24} \sim \frac{7}{24}, \frac{17}{24} \sim \frac{19}{24}$, $\frac{23}{96} \sim \frac{25}{96}$, $\frac{71}{96} \sim \frac{73}{96}$... (in general $\frac{1}{4} - \frac{1}{6 \cdot 4^m} \sim \frac{1}{4} + \frac{1}{6 \cdot 4^m}$, $\frac{3}{4} - \frac{1}{6 \cdot 4^m} \sim \frac{3}{4} + \frac{1}{6 \cdot 4^m}$). The horizontal strips and segments are shown in Figure 5.5.
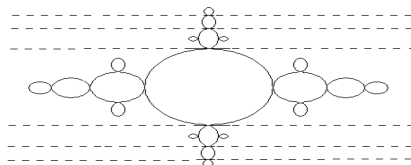

FIGURE 5.5

The vertical segments are also clearly visible in the C parameter space in Figure 2.2. Note that R_H preserves the central vertical segment and permutes the other vertical segments in left-right pairs, while R_V preserves all vertical segments. Similarly, R_V preserves the central horizontal segment and permutes the other horizontal segments in up-down pairs, while R_H preserves all horizontal segments.

In the general cases, the central vertical segment corresponds to the pair of intervals $[\frac{1}{2(2^k-1)}, \frac{1}{2^k-1}]$ and $[\frac{1}{2} + \frac{1}{2(2^k-1)}, \frac{1}{2} + \frac{1}{2^k-1}]$ between the points of V_1'. Each time we subdivide a loop we add a vertical segment corresponding to the pair of small intervals at the ends of the loop. In terms of $\mathcal{J}$, a vertical segment contains a circle together with all loops that join it except at the midpoints. Similarly, a horizontal segment contains a circle together with all loops that join it except at the midpoints. In particular, the central horizontal segment in C parameters is just the complement of the two intervals $[\frac{2^k+1}{2^{k+1}(2^k-1)}, \frac{2^{k+1}-1}{2^{k+1}(2^k-1)}]$ and $[\frac{1}{2} + \frac{2^k+1}{2^{k+1}(2^k-1)}, \frac{1}{2} + \frac{2^{k+1}-1}{2^{k+1}(2^k-1)}]$. Again R_H preserves the central vertical segment and permutes the other vertical segments in pairs, etc.

Theorem 5.1. *Let u be an eigenfunction of Δ_μ that is odd with respect to R_H (resp. R_V). If $\tilde{u}$ is the restriction of u to any horizontal (resp. vertical) segment, defined to be equal to zero outside that segment, then $\tilde{u}$ is also an eigenfunction. In particular, if λ is any primitive eigenvalue of multiplicity 1, then the corresponding eigenfunction is supported on the central horizontal or vertical segment, depending on its H or V type.*

Proof. The eigenvalue equation for $\tilde{u}$ is obvious at all points except the endpoints of the segment. Because u is odd, $\tilde{u}$ vanishes at the endpoints. This also implies $\Delta_\mu \tilde{u}$ is zero at the endpoints. Thus the eigenvalue equation is trivially true at the endpoints ($0 = \lambda 0$). If the multiplicity of the eigenvalue is 1, u must vanish identically on all but one segment. If this were not a central segment, then we could obtain a linearly independent eigenfunction by composing u with one of the reflections. $\square$

We will give more applications of this result in section 7.

6. NUMERICAL DATA

1. Conformal measure.

   We present numerical results relevant to the computation of ν. As Hausdorff dimension is used in (4.6) to derive ν its computation is given for each of the examples we will discuss: 2 quasicircles ($c = .2$ and $c = .33 - .25i$), the standard basilica ($c = -1$), one other $k = 2$ type Julia set ($c = -1 + .15i$) and the standard rabbit ($c = -.122 + .745i$). To help build intuition we give the conformal measure, the corresponding cumulative distribution function, and $J'(z) = 2|z|$ on the standard basilica. For more computational results see [Flo08].

   (i.) Computation of Hausdorff dimension d.

   To approximate the Hausdorff dimension of the Julia set corresponding to $z^2 + c$ we calculate the sum of weights assigned by equation (4.6) for d chosen at regular intervals in $[1, 2]$ on graph levels 1-22 (1-21 in the case of rabbit). If d is chosen too large, the sequence will diverge, and for d too small, the sequence tends to 0. Given this we refine the grid. Continuing this process allows us to estimate d to the desired accuracy. For $c = .2$ we estimate $d = 1.0257$, using the sequence of graphs in Figure 6.1.
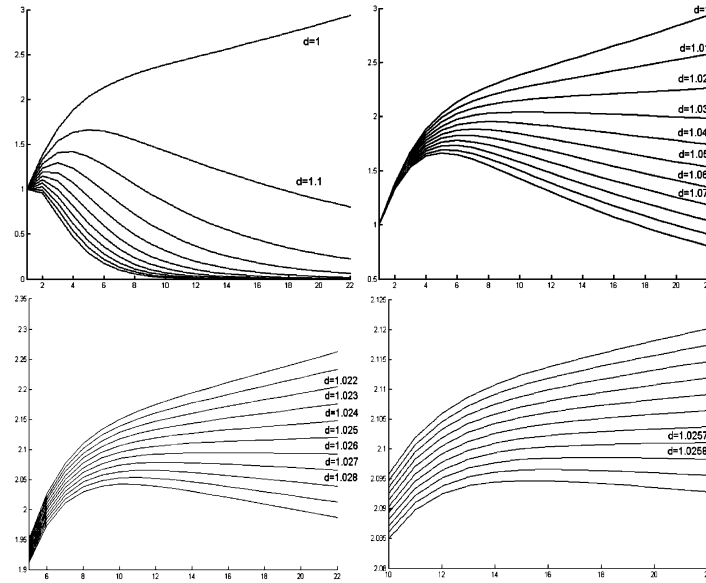
FIGURE 6.1. $c = .2$ **Ranges of d from top left to bottom right**: 1-2 in increments of .1, 1-1.1 by .01, d ranges 1.02-1.03 by .001, 1.025-1.026 by .0001.

   For $c = .33 - .25i$ we estimate $d = 1.1735$ in Figure 6.2.
   For the basilica, $c = -1$, we approximate $d = 1.2683$ in Figure 6.3.
   Next we examine $c = -1 + .15i$ and estimate $d = 1.3052$ in Figure 6.4.
   Next we examine $c = -.122 + .745i$, the rabbit. We estimate $d = 1.39$ in Figure 6.5. Because of the cycles in data, we would need greater computational power to improve this estimate.
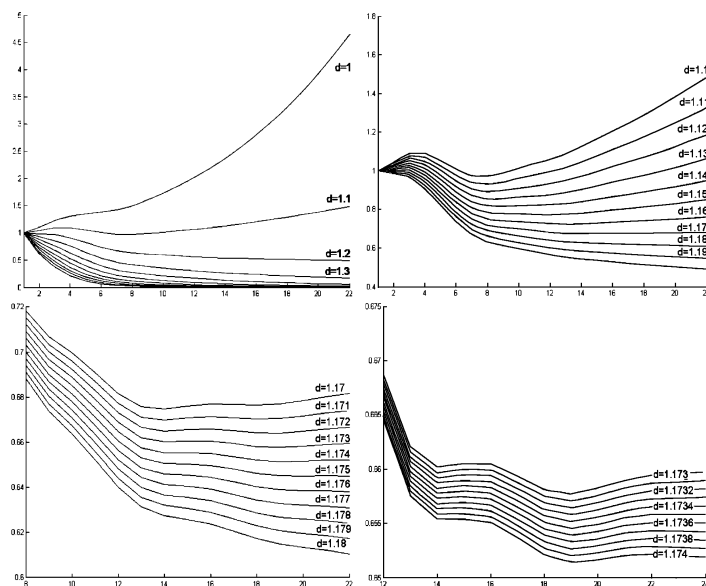
FIGURE 6.2. $c = .33 - .25i$ **Ranges of** d **from top left to bottom right**: 1-2 in increments of .1, 1.1-1.2 in increments of .01, 1.17-1.18 in increments of .001, 1.173-1.174 in increments of .0001.
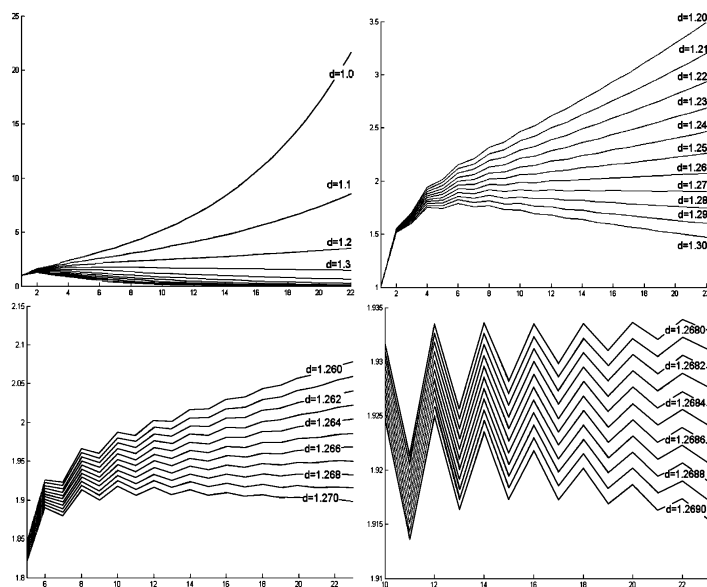
FIGURE 6.3. $c = . - 1$ **Ranges of** d **from top left to bottom right**: 1-2 in increments of .1, 1.2-1.3 in increments of .01, 1.26-1.27 in increments of .001, 1.268-1.269 in increments of .0001.

We note that these results correspond to our expectations. The Hausdorff dimension falls between 1 and 2, and increases as we increase
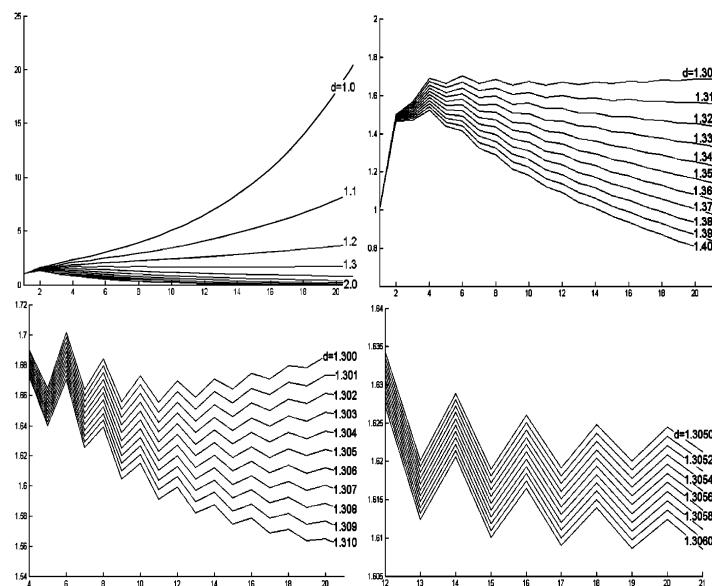
FIGURE 6.4. $c = -1 + .15i$ **Ranges of d from top left to bottom right**: 1-2 in increments of .1, 1.3-1.4 in increments of .01, 1.30-1.31 in increments of .001, 1.305-1.306 in increments of .0001.
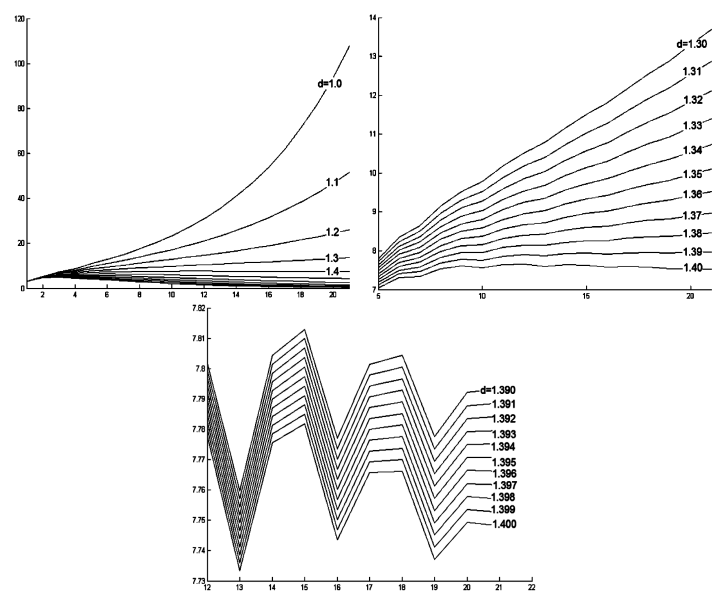
FIGURE 6.5. $c = -.122 + .745i$ **Ranges of d from left to right**: 1-2 in increments of .1, 1.3-1.4 in increments of .01, 1.39-1.40 in increments of .001.

topological complexity, and for the $k = 1$ and $k = 2$ examples the set that intutitively looks more complex in fact has a higher estimated Hausdorff dimension.

(ii.) Data relevant to the computation of ν on the standard basilica, using $d = 1.2683$.

Once we have an estimate of the Hausdorff dimension we use it to construct the conformal measure as in equation (4.6). This is pictured in Figure 6.6.
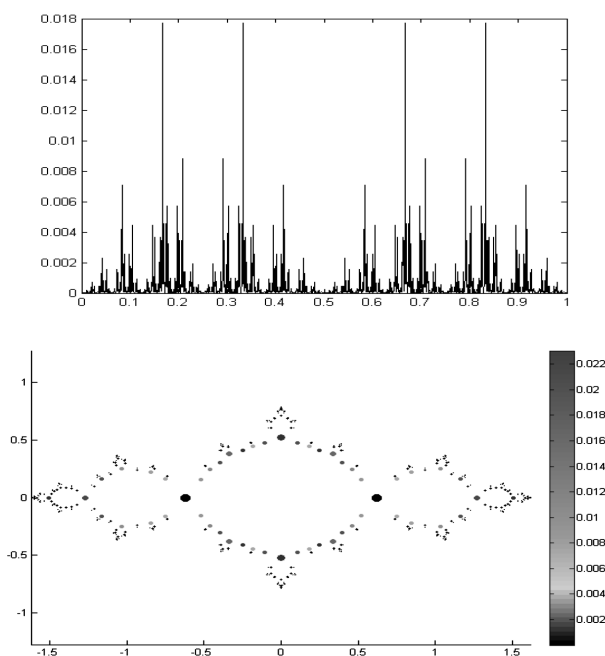
FIGURE 6.6. **Top:** ν with respect to ray parameterization. **Bottom:** approximation to ν by pointmasses.

We also give the cumulative distribution function for ν and the graph of $|J'(z)| = 2|z|$ as pointmasses (for comparsion to ν). This is shown in Figure 6.7.

2. Spectra - Equilibrium measure.

(i.) Computation of the spectra.

Our program is divided into two pieces. First we set up the problem by computing the m-th level graph approximation in C and in the ray parameter, as per the discussion in section 2, recording the appropriate identifications. We then calculate weights given the choice of measure. Using this information we construct the m-th level Laplacian matrix as in (1.11). We then use Matlab(R2007b)'s Eig function to find the
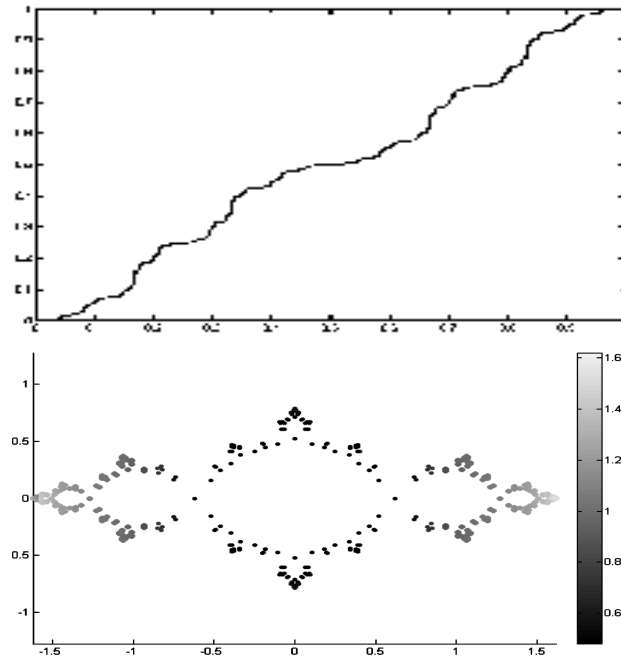
FIGURE 6.7. **Top:** $\nu([0, x])$. **Bottom:** approximation to $|J'(z)| = 2|z|$ by pointmasses.

eigenvalues and eigenvectors of our Laplacian matrix. These results are given below.

(ii.) Computed eigenvalues and eigenfunctions for the basilica $c = -1$ ($k = 2$).

In Table 1 we give the computed eigenvalues on the last four computed levels of the graph $(10 - 13)$, a predicted value, $D_n(Type_m)$, and $2^{3n/2} * \lambda_{Type_m}$. In Figure 6.9 there are pictures of the first 16 eigenfunctions as well as more detailed views of a few functions that show particularly interesting behavior.

We give the following for interpreting the tables. $D_n(Type_m)$, where $Type$ is V or H depending on whether the function is vertical or horizontal, m refers to the number of the primitive eigenfunction from which ours derives, and n is the number of derivations required to reach the current eigenfunction. $2^{3n/2} * \lambda_{Type_m}$ is the eigenvalue predicted by the P-invariance condition on Δ_μ given in (4.8). As the eigenvalue of $H1$ and $V1$ are known to have a high degree of accuracy, $2^{3n/2} * \lambda_{Type_m}$ will predict the eigenvalues of their derived eigenfunction with high accuracy. We then interpolate linearly between these values to obtain a prediction for arbitrary eigenfunctions. It should be noted that comparing eigenvalues predicted from the computation and by the equation $2^{3n/2} * \lambda_{Type_m}$ can alert us to approximation errors.

TABLE 1. Computed actual eigenvalues of Δ_μ $c = -1$

#	Level 10	Level 11	Level 12	Level 13	Predicted	$D_n(Type_m)$	$2^{3n/2} * \lambda_{Type_m}$
1	0	0	0	0	–	–	–
2	39.868	39.869	39.870	39.870	–	H1	–
3	112.757	112.765	112.768	112.769	112.769	D1(H1)	112.769
4	196.499	196.537	196.542	196.547	196.548	V1	–
5	274.985	275.045	275.060	275.068	275.071	H2	–
6	318.848	318.924	318.946	318.956	318.960	D2(H1)	318.960
7-8	555.662	555.784	555.890	555.905	555.918	D1(V1)	555.918
9	777.435	777.774	777.946	777.988	778.012	D1(H2)	778.010
10	821.559	821.962	822.145	822.196	822.225	H3	–
11	901.338	901.838	902.054	902.116	902.154	D3(H1)	902.154
12	1087.702	1088.651	1088.887	1089.006	1089.055	H4	–
13	1131.912	1132.953	1133.205	1133.335	1133.389	V2	–
14-16	1569.255	1571.648	1571.996	1572.294	1572.375	D2(V1)	1572.375
17	2195.019	2198.918	2199.878	2200.364	2200.499	D2(H2)	2200.544
18	2242.639	2246.649	2247.673	2248.172	2248.333	H5	–
19	2319.552	2323.720	2324.859	2325.378	2325.568	D1(H3)	2325.521
20	2430.056	2434.671	2435.908	2436.483	2436.705	V3	–
21	2501.764	2506.543	2507.895	2508.489	2508.744	H6	–
22	2544.471	2549.369	2550.784	2551.393	2551.678	D4(H1)	2551.678
23	3069.346	3074.711	3077.393	3078.061	3078.503	H7	–
24	3071.110	3076.486	3079.169	3079.838	3080.381	D1(H4)	3080.173
25-26	3195.816	3201.531	3204.476	3205.187	3205.856	D1(V2)	3205.554
27-32	4430.630	4438.524	4445.292	4446.275	4447.347	D3(V1)	4447.347
33	6186.513	6208.450	6219.478	6222.195	6223.763	D3(H2)	6224.079
34	6229.699	6252.139	6263.256	6266.035	6267.683	H8	–
35	6319.742	6343.141	6354.483	6357.380	6359.121	D1(H5)	6358.792
36	6377.333	6401.701	6413.067	6416.084	6417.911	V4	–
37	6480.064	6505.510	6517.154	6520.303	6522.231	H9	–
38	6534.651	6560.683	6572.474	6575.695	6577.712	D2(H3)	6577.565
39-40	6844.940	6873.236	6886.290	6889.789	6891.977	D1(V3)	6891.414
41	7045.133	7076.056	7089.575	7093.397	7095.727	D1(H6)	7095.079
42	7086.397	7117.912	7131.514	7135.409	7137.831	H10	–
43	7164.472	7196.852	7210.705	7214.706	7217.234	D5(H1)	7217.234
44	7376.824	7413.193	7427.195	7431.687	7434.383	H11	–
45	7432.363	7469.456	7483.616	7488.196	7491.006	V5	–
46	8619.797	8681.423	8696.596	8704.182	8707.556	D1(H7)	8706.070
47	8622.301	8683.944	8699.133	8706.721	8710.204	H12	–
48	8624.752	8686.412	8701.615	8709.206	8712.799	D2(H4)	8712.045
49-51	8971.421	9039.132	9055.298	9063.627	9067.478	D2(V2)	9066.677
52	11065.940	11185.447	11204.938	11219.571	11224.478	V6	–
53	11066.291	11185.804	11205.297	11219.931	11224.977	H13	–
54-64	12374.923	12531.714	12554.041	12573.185	12578.996	D4(V1)	12578.996

Eigenvalue counting functions $N(x)$ and Weyl ratios $W(x)$ of Δ_μ for $c = -1$ are illustrated in Figure 6.8.
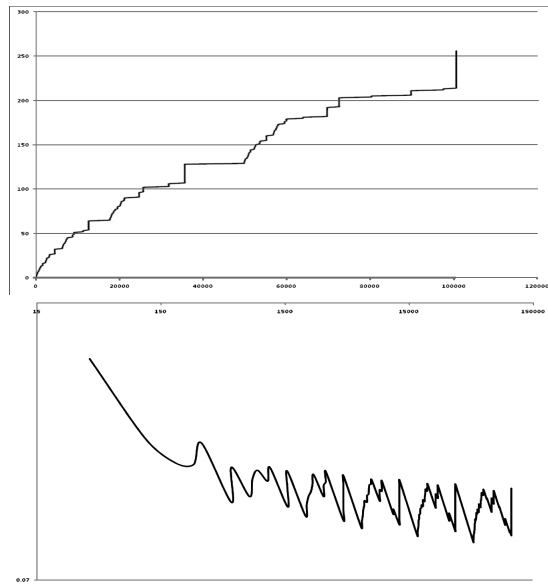
FIGURE 6.8. **Top:** Eigenvalue counting function and **Bottom:** Weyl ratio for predicted eigenvalues of Δ_μ for $c = -1$.

First 16 eigenfunctions for Δ_μ on the basilica $c = -1$. For "full graph" darker color represents positive values, lighter negative
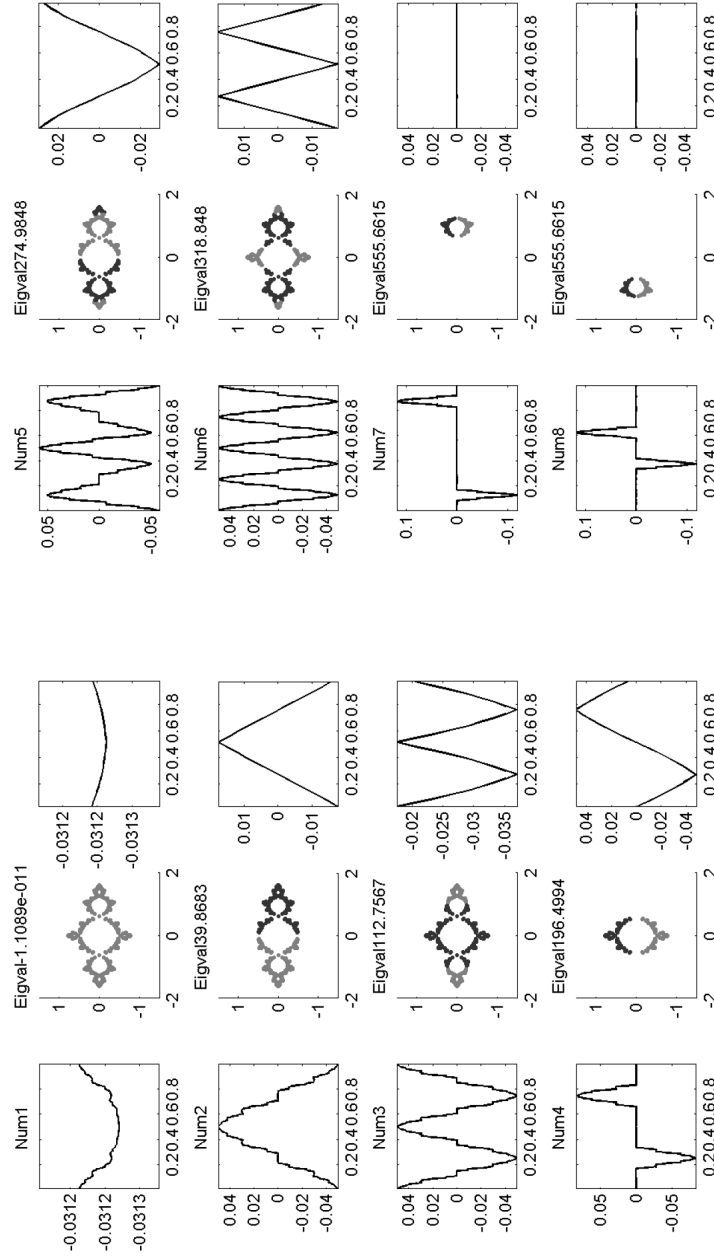
FIGURE 6.9. Eigenfunctions of Δ_μ for $c = -1$. Ray parameterization, full graph, inner circle
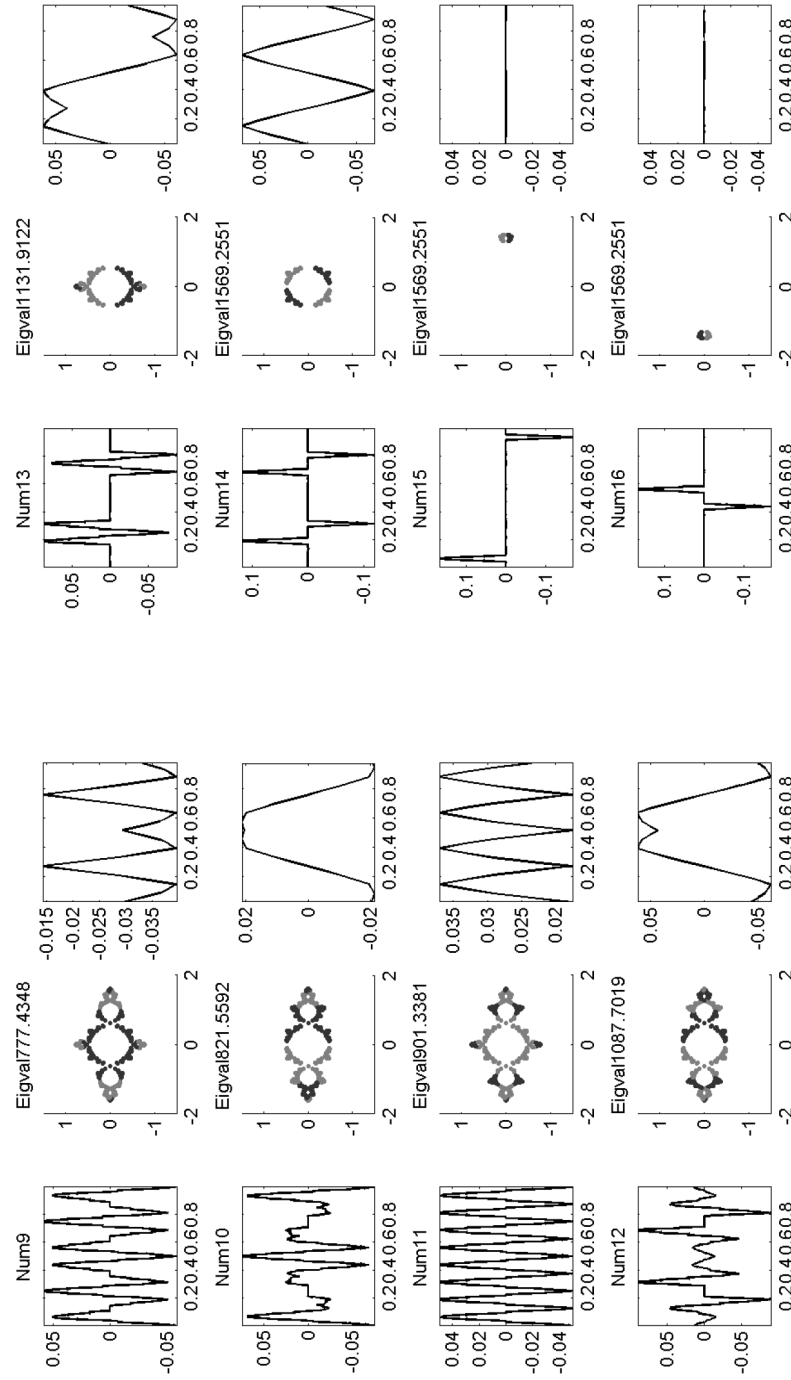
FIGURE 6.9 cont'd. Eigenfunctions of Δ_μ for $c = -1$. Ray parameterization, full graph, inner circle

(iii.) Computed eigenvalues and eigenfunctions for the rabbit $c = -.122 + i.745$ ($k = 3$).

For $c = -.122 + i.745$ we give the computed eigenvalues on several levels of the graph, a predicted value, $D_n(Type_m)$, and $2^{4n/3} * \lambda_{Type_m}$. The labeling scheme in Table 2 is the same as that in the previous table. $2^{4n/3} * \lambda_{Type_m}$ is the eigenvalue predicted by the P-invarience condition on Δ_μ given in (4.8). For Table 2, the predictions are based on the ratios of differences of successive terms, using the equation = $V + (D) * R/(1 - R)$ where V is the last computed value and D is the difference between V and the value at the prior level. As the ratios between successive differences oscillate with period 3, when there is sufficient data (namely for the first 32 eigenfunctions) we take R to be the average of the last 3 ratios. For $32 - 64$ we take R to be the ratio of two.

TABLE 2. Computed actual eigenvalues of Δ_μ $c = -.122 + .745i$

| #	Level 8	Level 9	Level 10	Level 11	Predicted	$D_n(Type_m)$	$2^{4n/3} * \lambda_{Type_m}$
1	0.000	0.000	0.000	0.000	0.000	–	–
2	165.721	165.824	165.883	165.904	165.923	H1	–
3	416.734	417.592	417.851	417.998	418.031	D1(H1)	418.052
4	511.495	512.956	513.414	513.584	513.724	H2	–
5	1044.099	1050.103	1052.266	1052.919	1053.731	D2(H1)	1053.424
6	1130.963	1137.403	1140.071	1140.884	1141.822	H3	–
7	1281.905	1288.888	1292.567	1293.721	1295.003	D1(H2)	1294.150
8	1714.862	1725.744	1733.302	1735.285	1738.810	V1	–
9	2461.466	2485.993	2499.697	2504.461	2508.700	H4	–
10	2603.427	2630.964	2646.093	2651.543	2655.987	D3(H1)	2654.462
11	2805.593	2839.746	2855.919	2862.590	2866.231	H5	–
12	2815.301	2849.849	2866.075	2872.798	2876.407	D1(H3)	2874.848
13	3151.277	3200.372	3217.576	3226.638	3228.738	H6	–
14	3180.544	3230.197	3247.793	3257.065	3259.212	D2(H2)	3261.054
15-16	4232.083	4321.182	4348.603	4367.648	4368.480	D1(V1)	4372.645
17	5984.182	6202.505	6264.310	6298.841	6303.698	D1(H4)	6310.847
18	6092.709	6321.151	6386.209	6421.640	6427.175	H7	–
19	6309.295	6560.226	6629.613	6667.737	6673.458	D4(H1)	6688.825
20	6421.773	6685.026	6758.788	6797.444	6804.497	H8	–
21	6764.448	7069.650	7155.712	7196.465	7207.290	D1(H5)	7213.276
22	6773.988	7080.199	7166.696	7207.502	7218.460	H9	–
23	6786.602	7094.113	7181.169	7222.056	7233.172	D2(H3)	7244.163
24	6988.374	7319.172	7416.793	7458.105	7473.183	V2	–
25	7309.903	7685.383	7798.488	7840.769	7862.147	H10	–
26	7532.884	7940.721	8064.431	8107.784	8133.227	D1(H6)	8130.618
27	7572.136	7986.284	8110.729	8154.747	8180.088	H11	–
28	7596.424	8014.467	8139.587	8183.926	8209.368	D3(H2)	8217.340
29-32	9795.501	10664.182	10888.697	10957.794	11022.945	D2(V1)	11018.375
33	13391.179	15079.194	15629.334	15785.073	15870.193	D2(H4)	15902.339
34	13478.796	15187.726	15748.620	15907.468	15995.592	H12	–
35	13607.028	15352.665	15928.303	16092.240	16183.641	D1(H7)	16181.519
36	13687.105	15462.125	16050.142	16214.973	16309.161	H13	–
37	14014.754	15898.428	16530.733	16705.579	16809.660	D5(H1)	16854.782
38	14082.089	15979.695	16621.093	16798.785	16905.929	H14	–
39	14250.885	16181.855	16845.211	17031.078	17145.843	D1(H8)	17128.485
40	14708.995	16744.411	17478.016	17681.173	17821.144	V3	–

TABLE 2. Computed actual eigenvalues of Δ_μ $c = -.122 + .745i$

#	Level 8	Level 9	Level 10	Level 11	Predicted	$D_n(Type_m)$	$2^{4n/3} * \lambda_{Type_m}$
41	14834.130	16889.618	17640.765	17850.884	17998.458	H15	–
42	14959.402	17045.341	17814.402	18031.263	18185.257	D2(H5)	18176.317
43	14977.379	17068.516	17840.036	18057.965	18212.708	H16	–
44	14977.979	17069.379	17840.983	18058.943	18213.698	D1(H9)	18161.766
45	14987.186	17082.284	17855.123	18073.616	18228.584	H17	–
46	15001.932	17101.165	17876.044	18095.412	18251.028	D3(H3)	18254.146
47-48	15416.746	17609.599	18443.159	18689.148	18868.023	D1(V2)	18793.248
49	16085.687	18419.802	19365.950	19650.959	19882.827	D1(H10)	19757.500
50	16281.024	18665.713	19648.130	19944.139	20192.717	H18	–
51	16525.107	18981.677	20009.364	20321.092	20589.538	D2(H6)	20487.873
52	16574.303	19050.999	20089.820	20403.281	20675.662	H19	–
53	16592.597	19080.588	20124.174	20437.758	20711.110	D1(H11)	20548.674
54	16597.938	19088.831	20133.808	20447.430	20721.151	H20	–
55	16636.257	19141.788	20195.192	20510.474	20787.384	D4(H2)	20706.400
56	17991.470	20860.052	22227.106	22606.649	23054.707	H21	–
57	18220.720	21192.118	22619.110	23012.838	23486.608	V4	–
58-64	20748.808	24683.116	26872.054	27437.798	28376.990	D3(V1)	27764.564

Eigenvalue counting functions $N(x)$ and Weyl ratios $W(x)$ of Δ_μ for $c = -.122 + 754i$ are illustrated in Figure 6.10.
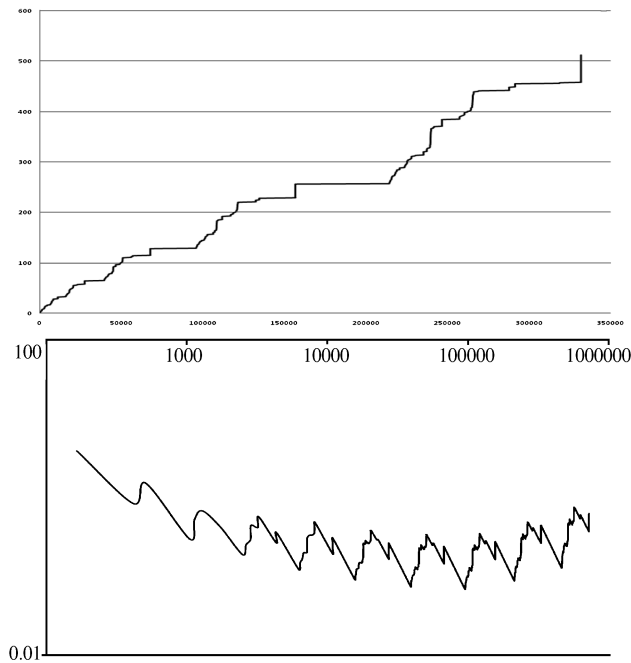
FIGURE 6.10. **Top:** Eigenvalue counting function. **Bottom:** Weyl ratio for level 10 eigenvalues of Δ_μ for $c = -.122 + 754i$.

First 16 eigenfunctions for Δ_μ on the rabbit $c = -.122 + 754i$
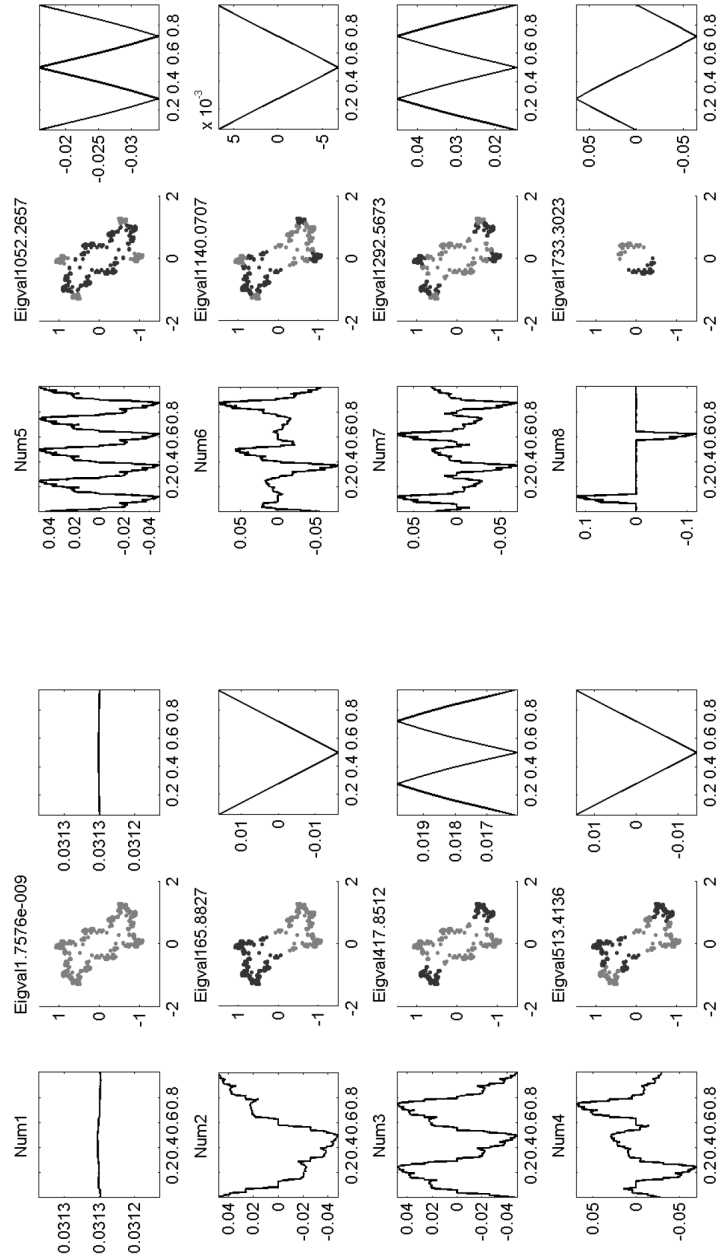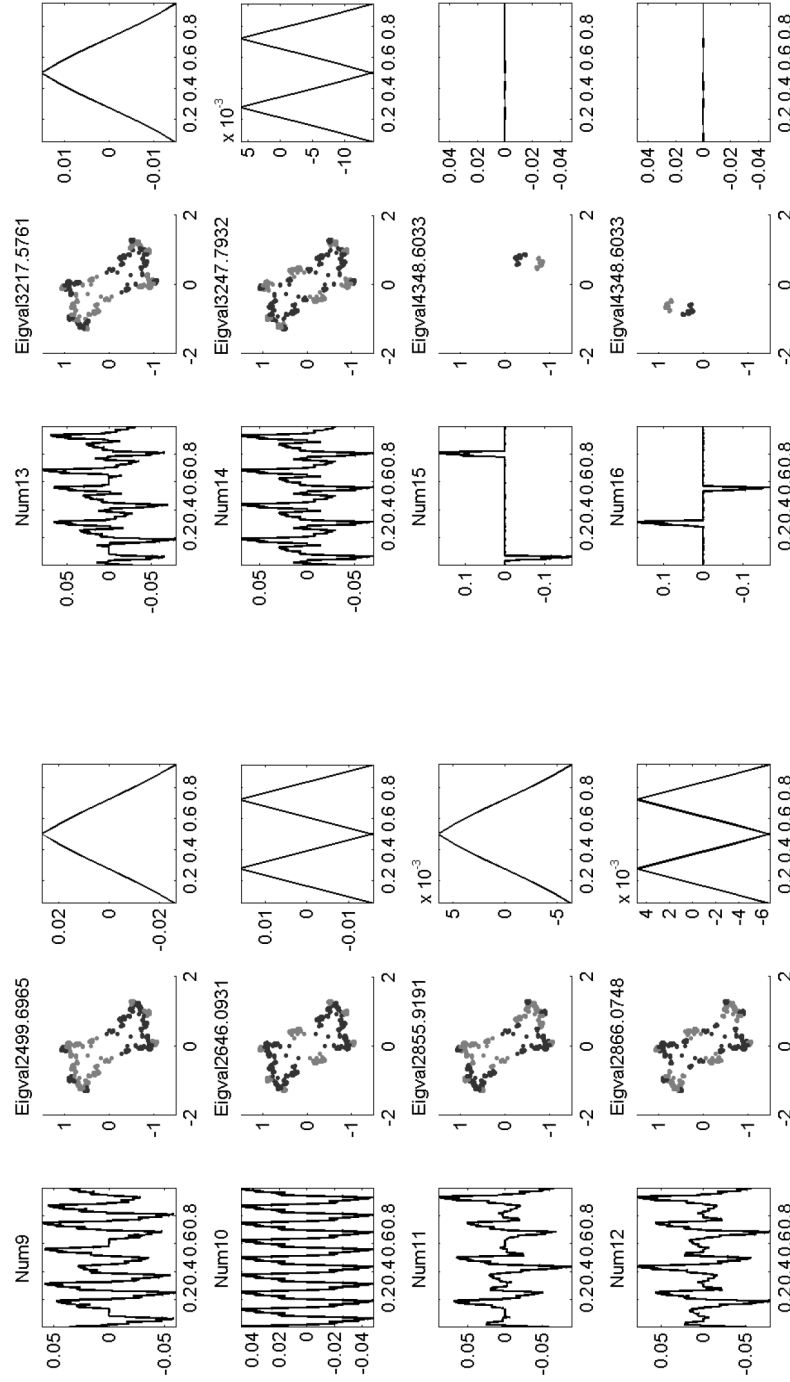
FIGURE 6.11. Eigenfunctions of Δ_μ for $c = -.122 + 754i$. *Ray parameterization, full graph, inner circle*

FIGURE 6.11 cont'd. Eigenfunctions of Δ_μ for $c = -.122 + 754i$. Ray parameterization, full graph, inner circle

3. Computed eigenvalues for conformal measure.
   (i.) Spectrum of Δ_ν for $c = .33 - i.25$.

TABLE 3. Computed actual eigenvalues of Δ_ν $c = .33 - i.25$

#	Level 6	Level 7	Level 8	Level 9
1	0	0	0	0
2	32.147045	32.493944	33.28344	33.567551
3	48.213964	46.998041	45.831625	45.762296
4	122.46591	117.836174	120.090215	124.059287
5	221.515707	229.782687	217.016349	207.709143
6	348.275565	349.237686	336.490519	334.507733
7	402.528864	398.717183	382.160799	377.698993
8	536.065552	513.365788	488.130227	493.410108
9	876.420583	963.36787	974.702375	907.075854
10	1038.939947	1081.255888	1074.177368	1015.481251
11	1196.992559	1324.534496	1339.064483	1258.409975
12	1432.349755	1505.609269	1499.557881	1415.362104
13	1671.287945	1844.610709	1820.091867	1725.159848
14	1931.736137	2084.511213	2022.130546	1901.094616
15	2160.282968	2271.38594	2210.748616	2097.581584
16	2390.670583	2470.446017	2349.046872	2207.099921
17	2862.214873	3102.18503	3204.397413	3132.506021
18	3032.334758	3183.224372	3240.198287	3155.133143
19	3653.187355	4644.951507	4987.653933	4965.215177
20	3891.907398	4802.664106	5055.47932	5007.433061
21	4087.049651	5244.542959	5845.797103	5916.637283
22	4310.870181	5609.431657	6072.135662	6109.213514
23	4967.917359	5919.356572	6483.155425	6418.244519
24	5071.33176	6372.640313	6811.332993	6679.5298
25	5773.539558	6781.306359	7446.945858	7525.924043
26	5832.680903	7140.958951	7726.339165	7760.311456
27	6782.990767	7855.556304	8626.395028	8372.994018
28	6819.313619	8073.902679	8845.912587	8569.213931
29	7438.732021	9076.598872	9907.017257	9747.808669
30	7459.725171	9202.458558	10099.96723	9888.987375
31	8682.40089	10542.16847	11075.34404	10592.24438
32	8688.625395	10636.58729	11237.03472	10693.5242
33	9706.177386	11569.0098	12105.03168	11643.80223
34	9709.708534	11634.02093	12183.30804	11671.35646
35	10667.63625	13696.86614	14912.61044	15009.53452
36	10669.67764	13756.49353	14939.97457	15012.16227
37	11260.96297	14359.76031	16166.92427	17851.6214
38	11261.7744	14410.78132	16188.82351	17853.97145
39	13198.53503	16700.91335	19154.70775	21239.4282
40	13198.58502	16720.31099	19166.86589	21246.03279
41	14397.21269	17906.69673	22138.63227	23102.63183
42	14397.23309	17922.7418	22171.82231	23116.20459
43	15220.09027	19957.69527	24061.96944	25736.81951
44	15220.09613	19967.32679	24169.75053	25770.33133
45	18243.17265	21406.46536	25400.54444	27843.78249
46	18243.17296	21413.48319	25578.78226	27986.64662
47	19102.51281	23502.95745	26913.93495	28601.6936
48	19102.51305	23506.96232	27079.28317	28754.16174
49	19829.69063	25694.10826	28724.18477	30793.53445
50	19829.6907	25700.05814	28827.45876	30841.63357
51	22783.03703	26547.81827	31383.84427	34134.31846
52	22783.03703	26553.31359	31466.70217	34161.15367
53	23433.84958	28213.6788	33262.0093	37167.81211
54	23433.84958	28215.58649	33403.19865	37198.58281
55	25351.5334	29443.75655	33931.28181	40833.49261
56	25351.5334	29444.3795	34027.61129	40929.61047
57	27715.38255	33742.34761	40150.23673	42690.50214
58	27715.38255	33742.47023	40197.5881	43007.41972
59	30187.97798	34487.14396	40653.53005	43539.05115
60	30187.97798	34487.24285	40704.6437	43816.15511
61	30433.62543	38115.29114	43793.17644	46847.27639
62	30433.62543	38115.31519	43808.84607	46912.24644
63	32301.2602	39168.36533	45119.54855	49225.86082
64	32301.2602	39168.38327	45129.02125	49257.94419

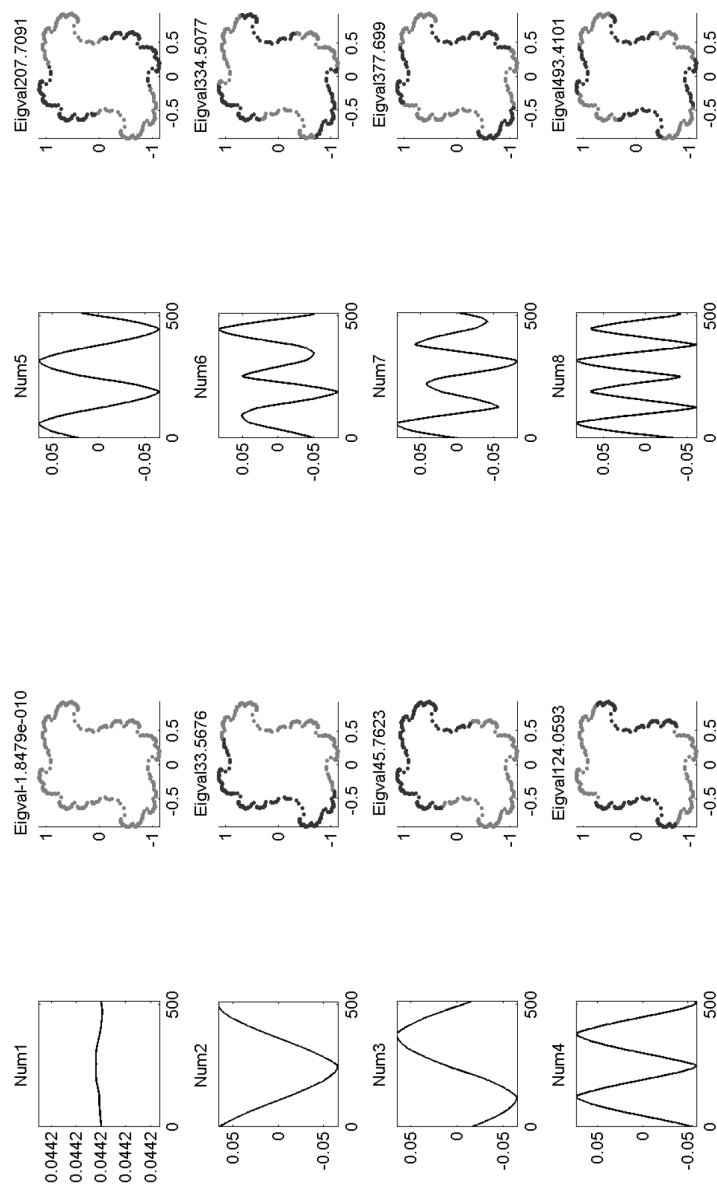First 8 eigenfunctions for Δ_ν for $c = .33 - i.25$

FIGURE 6.12. Eigenfunctions of Δ_ν for $c = .33 - i.25$. Ray parameterization, full graph, inner circle

(ii.) Spectrum of Δ_ν for $c = -1$

TABLE 4. Computed actual eigenvalues of Δ_ν $c = -1$

#	Level 9	Level 10	Level 11	Level 12	Level 13
1	0	0	0	0	0
2	60.993	59.761	60.776	59.949	60.628867
3	182.781	184.375	183.037	184.066	183.189141
4	250.142	254.048	250.815	253.467	251.225964
5	408.589	416.593	412.107	416.718	413.460382
6	607.593	598.198	608.204	601.322	607.494978
7	937.63	901.597	930.195	905.794	925.308868
8	937.63	901.597	930.195	905.794	925.308868
9	1022.231	1029.651	1024.59	1028.42	1025.052159
10	1160.736	1161.321	1166.692	1164.51	1167.417114
11	1347.226	1413.452	1361.854	1403.747	1368.444548
12	1565.244	1581.749	1568.929	1578.585	1569.386446
13	2071.629	2027.882	2086.665	2050.588	2085.253372
14	2108.431	2059.044	2127.713	2086.337	2126.473126
15	2698.402	2748.683	2759.452	2776.753	2775.995933
16	2773.467	2822.446	2847.363	2860.13	2866.581565
17	3958.772	4236.727	4115.627	4272.308	4163.937776
18	4109.522	4236.727	4226.164	4281.382	4255.618846
19	4496.357	4261.632	4453.202	4281.382	4418.306492
20	4496.357	4286.489	4453.202	4305.384	4418.306492
21	4804.91	4973.398	4832.476	4938.417	4844.527057
22	4804.91	4973.398	4832.476	4938.417	4844.527057
23	5043.498	5167.456	5164.223	5190.534	5182.9662
24	5299.332	5320.95	5399.135	5357.508	5401.490376
25	5580.047	5597.046	5600.197	5604.838	5599.106515
26	5639.196	5748.875	5760.21	5807.467	5798.602469
27	6059.609	6120.725	6332.735	6159.407	6295.939516
28	6368.979	6120.725	6332.735	6159.407	6295.939516
29	6368.979	6835.93	6445.912	6786.398	6521.592066
30	6687.094	7258.7	7094.039	7280.802	7156.022336
31	8032.96	8759.128	8643.513	8934.386	8767.016104
32	8760.168	9213.677	9169.495	9352.056	9219.785067

Eigenvalue counting functions $N(x)$ and Weyl ratios $W(x)$ of Δ_ν for $c = -1$ are illustrated in Figure 6.13.
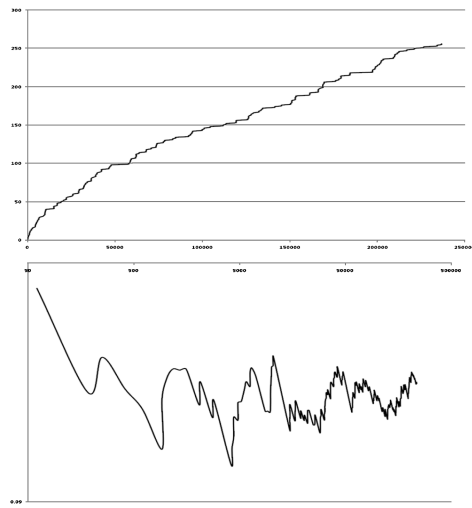
FIGURE 6.13. **Top:** Eigenvalue counting function.   **Bottom:** Weyl ratio for level 13 eigenvalues of Δ_μ for $c = -1$.
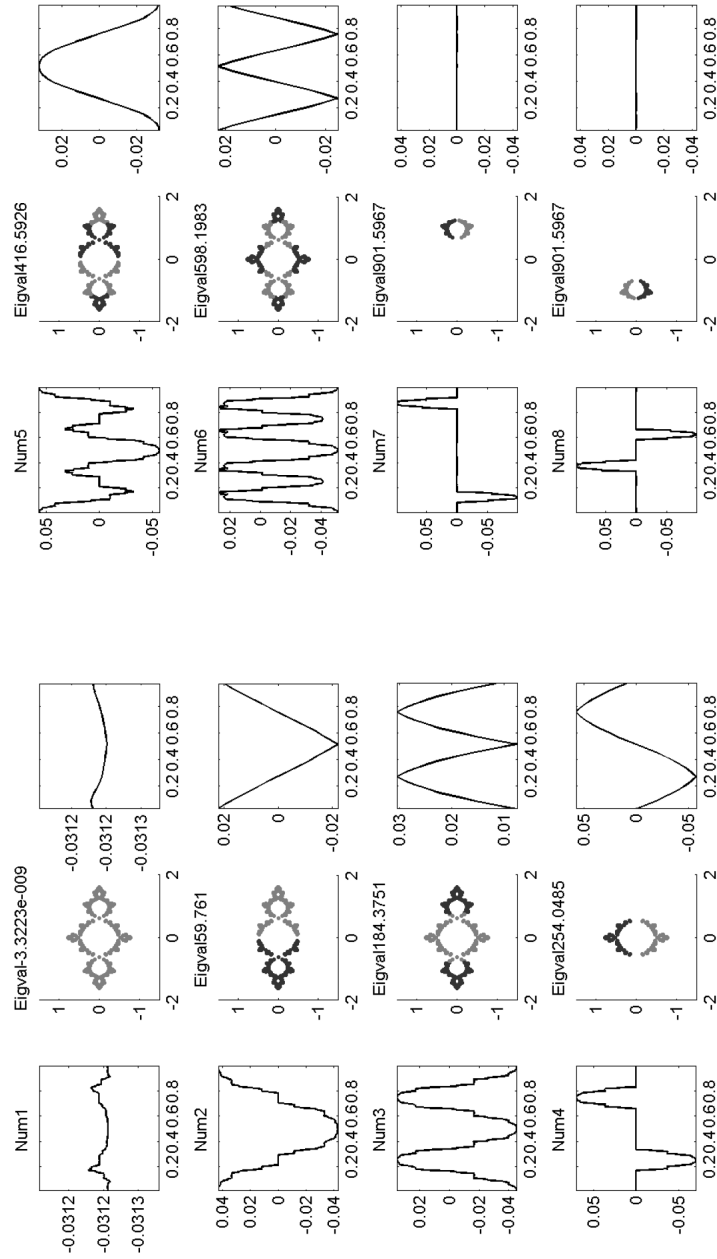
First 8 eigenfunctions for Δ_ν for $c = -1$

FIGURE 6.14. Eigenfunctions of Δ_ν for $c = .-1$. *Ray parameterization, full graph, inner circle*

(iii.) Spectrum of Δ_ν for $c = -.122 + .745i$

TABLE 5. Computed actual eigenvalues of Δ_ν c=-.122+754i

#	Level 7	Level 8	Level 9	Level 10
1	0	0	0	0
2	261.008937	256.664994	253.711999	259.52622
3	813.033353	835.841454	818.641623	816.925874
4	1050.51323	1090.320889	1050.878724	1063.443478
5	1864.503404	1905.595532	1892.242852	1857.100836
6	1932.097398	1996.110259	2032.413754	1954.662605
7	2961.599964	2959.060298	3046.176418	3071.876939
8	3556.548564	3414.215759	3472.053116	3546.823528
9	4403.60581	4527.32098	4691.691621	4634.515807
10	4717.04317	4850.516649	5024.370658	5072.002514
11	6084.753065	5515.328777	5643.478349	5826.623251
12	6138.707034	5540.670949	5671.383262	5881.593203
13	6699.292031	7542.517574	7719.424833	7724.245096
14	7090.00968	7732.659114	7854.390363	7965.143787
15	7754.620735	11083.54177	12206.02323	11921.05164
16	8059.503222	11769.58648	12345.74849	11992.92658

Because of the large differences in weight between points of a given level (as seen in Figure 6.10), our computational methods lose accuracy in this case.

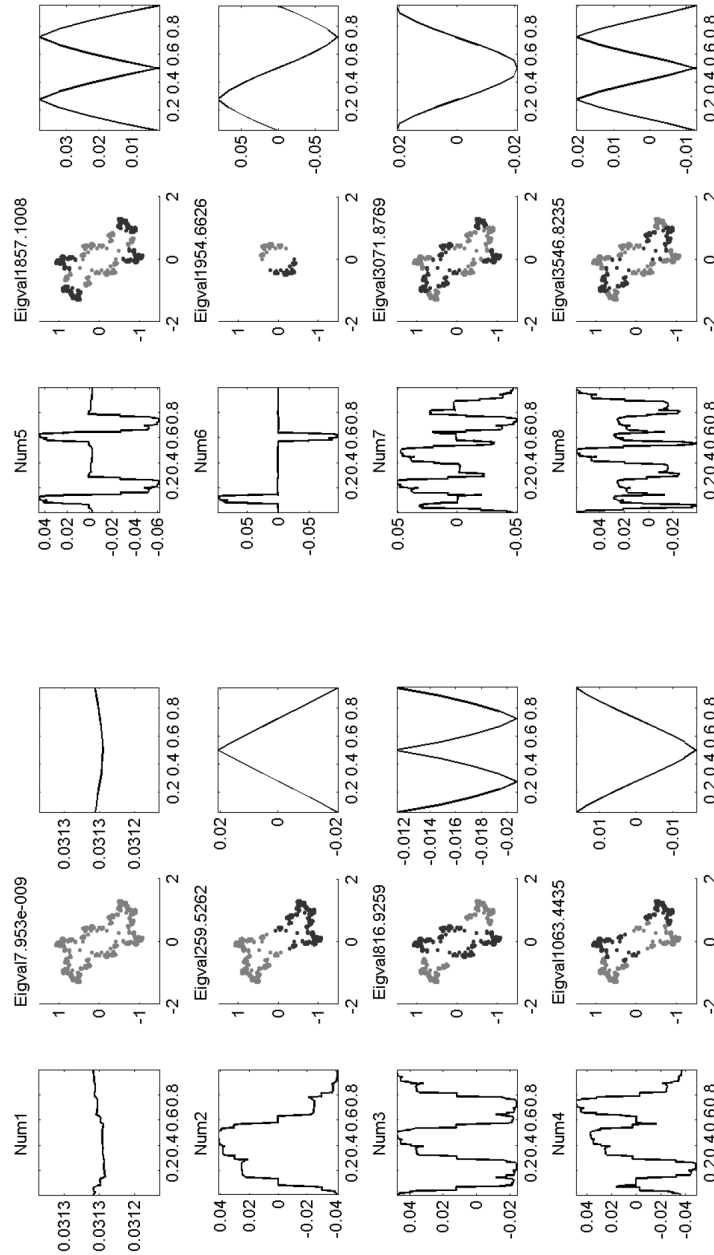First 8 eigenfunctions for Δ_ν for Douady's rabbit, $c = -.122 + .745i$

FIGURE 6.15. Eigenfunctions of Δ_ν for $c = .33 - i.25$. Ray parameterization, full graph, inner circle

7. Structure of the spectrum

There is obviously a great deal of structure to the spectrum of the equilibrium Laplacian Δ_μ. As noted in [RT09] for the basilica, the eigenvalue counting function has the asymptotic behavior

(7.1)
$$N(t) \sim t^{\frac{k}{k+1}} \ \text{ as } \ t \to \infty,$$

and moreover the Weyl ratio $W(t) = \frac{N(t)}{t^{\frac{k}{k+1}}}$ approaches a multiplicatively periodic function

(7.2)
$$W(t) = \varphi(t) + o(t) \ \text{ as } \ t \to \infty$$

with

(7.3)
$$\varphi(2^{1+\frac{1}{k}}t) = \varphi(t).$$

Here φ is bounded and bounded away from 0. This follows from results of [KL93] in the general case by the same argument as in [RT09]. Informally, if we compare the eigenfunction $u(x)$ and $u(2x)$, then we double the number of eigenvalues and multiply the eigenvalue by $2^{1+\frac{1}{k}}$ and by $2^{(1+\frac{1}{k})(\frac{k}{k+1})} = 2$. We see this asymptotic periodic behavior in the graphs of $W(t)$ in Figures 6.8 and 6.10. In contrast, Figure 6.13 shows that this is not the case for the conformal Laplacian. The data suggests the following:

Conjecture 7.1. *If λ is an eigenvalue of Δ_μ, then*

(7.4)
$$N(2^{1+\frac{1}{k}}\lambda) = 2N(\lambda) \quad or \quad 2N(\lambda) - 1.$$

Note that $N(\lambda)$ is the number of the last eignfunction in the λ-eigenspace. For example, for the basilica $\lambda_4 = 196.54\ldots$, $\lambda_7 = \lambda_8 = 555.89 \approx 2^{\frac{3}{2}}\lambda_4$, $\lambda_{14} = \lambda_{15} = \lambda_{16} = 1572 \approx 2^3\lambda_4$, $\lambda_{27},\ldots,\lambda_{32} = 4445.29 \approx 2^{\frac{9}{2}}\lambda_4$, $\lambda_{54},\ldots,\lambda_{64} = 12554.04 \approx 2^6\lambda_4$, $\lambda_{107},\ldots,\lambda_{128} = 35445.04 \approx 2^{\frac{15}{2}}\lambda_4$, $\lambda_{214},\ldots,\lambda_{256} = 98999.38 \approx 2^9\lambda_4$. Also, $\lambda_{13} = 1133.2,\ldots$, $\lambda_{25} = \lambda_{26} = 2^{\frac{3}{2}}\lambda_{13}$, $\lambda_{49} = \lambda_{50} = \lambda_{51} = 9.055.3 \approx 2^3\lambda_{13}$, $\lambda_{97},\ldots,\lambda_{102} = 25566.53 \approx 2^{\frac{9}{2}}\lambda_{13}$ $\lambda_{193},\ldots,\lambda_{203} = 71771.37 \approx 2^6\lambda_{13}$. In the first sequence we always have $N(2^{\frac{3}{2}}\lambda) = 2N(\lambda)$, while the second sequence alternates between that and $N(2^{\frac{3}{2}}\lambda) = 2N(\lambda) - 1$.

We can speculate some more as to when the two alternatives in (7.4) occur. Suppose λ is a primitive H eigenvalue. Then the values $N(2^{(1+\frac{1}{k})j}\lambda) = b_j$ will follow the pattern $b_{j+1} = 2b_j - \epsilon_j$ ($\epsilon_j = 0$ or 1) with ϵ_j periodic of period k. Moreover, $(\epsilon_0, \epsilon_1, \ldots, \epsilon_{k-1})$ will depend on $\#(\lambda) mod\ 2^k$. Table 7.1 shows the correspondence for $k = 2$ and 3.

For λ a primitive V eigenfunction a similar statement holds, but the correspondence is different. We don't have a lot of data, but it appears that $b_j = 2^j b_0$ when $\#(\lambda) \equiv 0\ mod\ 2^k$. We note that eigenvalue #53 for the basilica is a primitive eigenvalue of H type, but its derived spaces have multiplicities equal to a V type, and its ϵ sequence is $(0, 1)$, which is the same as for V types.

Assuming the above is correct, we may compute values for the Weyl ratio $W(2^{(1+\frac{1}{k})j})\lambda$ and $\varphi(\lambda)$ for these eigenvalues. For example, λ_{2^k} is the first primitive V eigenvalue, with $N(2^{(1+\frac{1}{k})j}\lambda_{2^k}) = 2^j 2^k$ and $W(2^{(1+\frac{1}{k})j}\lambda_{2^k}) = \frac{2^k}{\lambda_{2^k}^{(\frac{k}{k+1})}} = \varphi(\lambda_{2^k})$.

TABLE 7.1. $(\epsilon_0, \epsilon_1, \ldots, \epsilon_{k-1})$ given $\#(\lambda) mod\, 2^k$, $k = 2, 3$.

$\#(\lambda) mod\, 4$	(ϵ_0, ϵ_1)	$\#(\lambda) mod\, 8$	$(\epsilon_0, \epsilon_1, \epsilon_2)$
0	(0,0)	0	(0,0,0)
1	(1,1)	1	(1,1,1)
2	(1,0)	2	(1,0,0)
3	(0,1)	3	(1,0,1)
		4	(1,0,0)
		5	(0,1,1)
		6	(0,1,0)
		7(no data)	(0,0,1)

From the multiplicity formula in Theorem 7.3 we find

$$\varphi^-(\lambda_{2^k}) = \lim_{\epsilon \to 0^+} \varphi(\lambda_{2^k} - \epsilon) = \frac{2^k - \left(\frac{2^k - 2}{2^k - 1}\right)}{(\lambda_{2^k})^{\frac{k}{k+1}}}.$$

In Figures 6.8 and 6.10 we see these values as local maxima and minima. The same will be true for other primitive V eigenspaces, but quantitatively the effects may be much smaller. On the other hand, λ_2 is the first primitive H eigenvalue, with $N(2^{(1+\frac{1}{k})j}\lambda_2) = 2 \cdot 2^j$ and $W(2^{(1+\frac{1}{k})j}\lambda_2) = \frac{2}{\lambda_2}^{(\frac{k}{k+1})} = \varphi(\lambda_2)$, but this appears to be a local minimum, and similarly for the other primitive H eigenvalues.

Conjecture 7.2. *There are pairs of consecutive primitive eigenvalues (H_m, V_n) or (V_n, H_m) for every n and the appropriate m, and those are the only pairs of consecutive primitive eigenvalues. Then $D_j(H_m)$, $D_j(V_n)$ are consecutive eigenvalues for all j. In the case $n = 1$, $\lambda * 2^{k+j}$ is $D_j(V_1)$.*

We can explain the multiplicities as follows.

Theorem 7.3. *Let λ be a simple primitive eigenvalue associated to a V eigenfunction, and let $2^{n(1+\frac{1}{k})}\lambda$ be the n-th derived eigenvalue. Then the multiplicity $mult(2^{n(1+\frac{1}{k})}\lambda)$ of the eigenspace is at least*

$$(7.5) \qquad 2^j \left(2^{mk} - \frac{2^{mk} - 1}{2^k - 1}\right), \qquad n = mk + j, \; j = 0, 1, \ldots, k - 1.$$

Proof. The λ-eigenfunction $u(x)$ is supported in the vertical segment and has symmetry type $-+$. Then $u(2x)$ is supported in the two vertical segments that are separated by the central vertical segment, so we can restrict it to either vertical segment and still have an eigenfunction. Thus the multiplicity is at least 2 when $n = 1$. A similar argument shows that the number of vertical segments doubles as n increases up to $k-1$, since each vertical segment gets mapped to two distinct vertical segments under P^{-1}. In terms of the parameterization, the central vertical segment is the union of two intervals, $[\frac{1}{2(2^k-1)}, \frac{2}{2(2^k-1)}] \cup [\frac{2^k}{2(2^k-1)}, \frac{2^k+1}{2(2^k-1)}]$. After n iterations of P^{-1} this is mapped into the union of 2^{m+1} intervals $[\frac{1+l(2k-1)}{2^{n+1}(2^k-1)}, \frac{2+l(2k-1)}{2^{n+1}(2^k-1)}]$ for $0 \leq l < 2^{n+1}$. Note that these are exactly the shortest intervals in Γ'_{n+1}. For $n < k$ they pair up to give 2^n vertical segments. However, when $n = k$ there are $2^k - 2$ pairs of intervals that make up vertical segments, but the 4 intervals corresponding to $l = 1, 2, 2^k, 2^k + 1$ that lie in the central vertical segment form a single connected

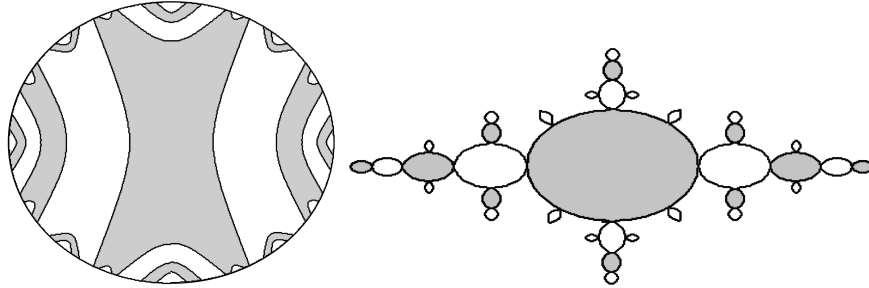region (in this case the intersection of the central vertical segment and the central horizontal segment).

FIGURE 7.1. **Left**: The 11 connected components for $k = 2$, $n = 4$.
Right: The corresponding regions on the basilica.

Thus the lower bound for multiplicity when $n = k$ is $2^k - 1$. The pattern then repeats, with

$$(7.6) \qquad \#(mk + j) = \begin{cases} 2\#(mk + j - 1) & \text{if } j = 1, \ldots, k - 1, \\ 2\#(mk + j - 1) - 1 & \text{if } j = 0, \end{cases}$$

where $\#(n)$ denotes the number of connected components in the support of $u(P^n x)$. See Figures 7.1 and 7.2. Then $\#(n)$ is given explicitly by (7.5). $\qquad \square$

There are few examples of eigenfunctions that display more complex behavior than outlined above, most notably 212-213 on the basilica. As the study of these examples is ongoing, more details may be found online [Flo08].

An immediate consequence of the high multiplicities in Theorem 7.3 is the following observation about the periodic function φ in the Weyl ratio (7.2).

Corollary 7.4. *The function φ in* (7.2) *is discontinuous; hence in particular it is not constant.*

Proof. Let λ be a simple primitive eigenvalue of V type. Then (7.5) implies $N(2^{n(1+\frac{1}{k})}\lambda) - N(2^{n(1+\frac{1}{k})}\lambda - \epsilon) \geq$ (7.5) for any $\epsilon > 0$. For simplicity take $n = mk$. Then $W(2^{m(k+1)}\lambda) - W(2^{m(k+1)}\lambda - \epsilon) \geq \frac{2^{mk} - \frac{2^{mk}-1}{2^k-1}}{(2^{m(k+1)}\lambda)^{\frac{k}{k+1}}} > \frac{2^{mk}(\frac{2^k-2}{2^k})}{2^{mk}\lambda^{\frac{k}{k+1}}}$, which implies that φ has a jump discontinuity at $t = \lambda$ of at least $(2^k - 2)2^{-k}\lambda^{-(\frac{k}{k+1})}$. $\qquad \square$

We may interpret the asymptotic behavior (7.1) as saying that $\mathcal{J}$ is a space of dimension k in the resistance metric and Δ_μ is an operator of order $k + 1$. The resistance metric $R(x, y)$ is defined by

$$(7.7) \qquad R(x, y)^{-1} = \inf \{\mathcal{E}(u, u) : u(x) = 0 \quad \text{and} \quad u(y) = 1\}.$$

While it is tricky to compute $R(x, y)$ exactly, it is not difficult to obtain order of magnitude estimates. We claim that if x and y are adjacent vertices in Γ_m, then $R(x, y)$ is comparable to $2^{-\frac{m}{k}}$. To see this we first observe that we can replace $\mathcal{E}$ by $\mathcal{E}^{(j)}$ in (7.7) because of the estimate (3.17). The function that achieves the minimum in (7.7) is the harmonic extension of u on V_m, so $\mathcal{E}^{(j)}(u, u) = \mathcal{E}_m(u, u) \geq 2^{\frac{m}{k}}$ (here $j \equiv m \mod k$) because of the contribution from the edge joining x and y. This gives
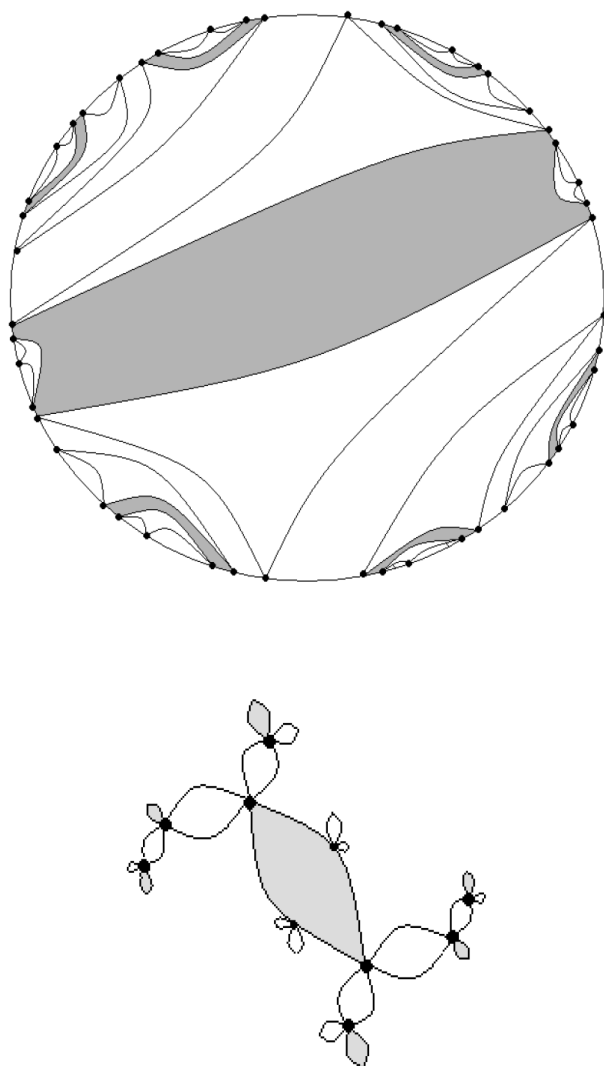
FIGURE 7.2. **Top:** The 7 connected components for $k = 3$, $n = 3$.
Bottom: The corresponding regions on the rabbit.

an upper bound for $R(x, y)$ of a multiple of $2^{-\frac{m}{k}}$, and we obtain a similar lower bound simply by filling in the values $u(z) = 0$ for all the other vertices $z \in V_m$.

The measure μ of the subset of $\mathcal{J}$ corresponding to the intervals in the parameter space connecting x and y is on the order of 2^{-m}. This translates into $\mu(B_r(x)) \sim r^k$, where $B_r(x)$ is the ball of radius r in the resistance metric centered at x. This says the measure μ is k-dimensional. We may cover $\mathcal{J}$ with a multiple of 2^m such subsets, each with diameter on the order of $2^{-\frac{m}{k}}$, and this can be used to show that $\mathcal{J}$ has box dimension and Hausdorff dimension k in the resistance metric.

Theorem 7.5. *Let λ be a primitive eigenvalue with an eigenfunction u of type H (resp. V). Then u is supported on the central horizontal (resp. vertical) segment.*

Proof. By symmetry we can restrict u to any horizontal (resp. vertical) segment and still obtain a λ-eigenfunction. If u is not supported in the central segment, then we can replace u by $\tilde{u}$ supported in a disjoint pair of segments that are permuted under R_V (resp. R_H). By symmetry we have $\tilde{u}(R_V x) = \tilde{u}(x)$ and $\tilde{u}(R_H x) = -\tilde{u}(R_H x)$ (resp. interchange R_V and R_H). We can then define yet another λ-eigenfunction by multiplying $\tilde{u}$ by -1 on one of the two segments. This eigenfunction has symmetry type $--$ and hence is derived, and this contradicts the assumption that λ is primitive. $\square$

Note that this theorem applies to primitive eigenfunctions of higer multiplicity. Since those spaces may have eigenfunctions that are linear combinations of H and V types, the theorem does not say anything about the supports of all primitive eigenfunctions. In section 8 we will show that the support of any eigenfunction cannot be all of $\mathcal{J}$.

Because of the rich structure of the eigenvalues and eigenfunction of Δ_μ, one is tempted to believe that some form of spectral decimation is present that would explain everything. While we cannot entirely rule this out, it is easy to see that spectral decimation does not hold for our sequence of graphs. Roughly speaking, spectral decimation would mean that eigenfunctions of the discrete Laplacians on Γ_m would extend to eigenfunctions of Δ_μ on $\mathcal{J}$, with eigenvalues changing in a predictable and monotonic fashion. However, the eigenfunctions on Γ_m for small m favor the $+-$ and $++$ types, since the points x of V'_m are mostly identified with $R_V x$. For example, for the basilica, there are no odd functions under R_V for $m = 1, 2$ and just 1 out of 8 for $m = 3$. But the data shows that eigenfunction 4 already has a $-+$ symmetry type. The situation is perhaps similar to the case of the pentagasket [ASST03]. We note that [RT09] describes a Laplacian on the basilica that does enjoy spectral decimation, but it is built from a different energy.

Two other features of the spectrum of the Laplacians (these are shared with Δ_ν) are apparent from the data: spectral gaps and spectral clusters. Spectral gaps mean there is a sequence $\{n_j\}$ with

$$(7.9) \qquad \frac{\lambda_{n_j+1} - \lambda_{n_j}}{\lambda_{n_j}} \geq r > 1.$$

In other words, not only is the gap between successive eigenvalues large, but it is large relative to the eigenvalues (this rules out the Laplacian on the sphere, for example). In fractals with spectral decimation, such as the Sierpinski gasket and the Vicsek set, it is possible to prove the existence of spectral gaps ([FS92], [Str06], [Zho09], [Zho10]). For the pentagasket, as here, there is only experimental evidence [ASST03]. Spectral gaps seem to occur right after derived vertical eigenspaces.

Spectral clustering is the phenomenon of distinct eigenvalues being very close. In its extreme form, which we believe holds in our case, it would say

(7.10) $\forall n \forall \epsilon > 0 \, \exists$ *an interval I of length ϵ containing n distinct eigenvalues.*

For example, in the basilica between eigenfunction 185-189 there are 3 distinct eigenvalues in the interval $[68978.39921, 68978.42095]$ of length $.02174$. One is tempted to suppose that this might be a single eigenspace with the differences in eigenvalues due to a combination of round-off errors and the inaccuracy due to

the approximation process. However, the data remains consistent over several levels
of approximation, so we are inclined to believe the eigenvalues are indeed distinct.
In the case of the Vicsek set, spectral clustering will be proved in [CSW09]. It does
not hold for the Sierpinski gasket. Experimental evidence in [ASST03] suggests
that it holds for the pentagasket.

In contrast to the equilibrium Laplacian, the conformal Laplacians Δ_ν do not
exhibit the same amount of spectral structure. Nevertheless, there are some in-
teresting features that we should mention. First we discuss two examples of qua-
sicircles, whose eigenfunctions are displayed in Figure 6.12 ($c = .33 - i.25$) and
online ($c = .24$) [Flo08] . In the case of the ordinary circle ($c = 0$), after the trivial
0-eigenspace of constants the eigenspaces have multiplicity 2 with eigenfunctions
$cos2\pi kx$ and $sin2\pi kx$ with eigenvalue $(2\pi k)^2$. In both examples the eigenfunctions
(in external ray parameterization) look like perturbations of the sines and cosines,
at least for small values of k. But the multiplicity 2 eigenspaces are replaced by
pairs of multiplicity 1 eigenspaces. In the second example, the horizontal and verti-
cal reflections in the parameter space preserve $|z|$ on $\mathcal{J}$, hence they are symmetries
of the measure ν and thus of Δ_ν as well. So each eigenfunction is either symmet-
ric or skew-symmetric under each symmetry. When k is odd the eigenspaces are
symmetric/skew-symmetric and skew-symmetric/symmetric, while when k is even
the eigenspaces are symmetric/symmetric and skew-symmetric/skew-symmetric.
There does not seem to be a pattern to predict which of the two has the lower
eigenvalue. In the first example there are no longer horizontal and vertical symme-
tries, only $z \to -z$ ($t \to t + \frac{1}{2}$ in the ray parameterization). Nevertheless the first
few eigenfunctions closely resemble the sines and cosines.

The eigenfunctions of the conformal Laplacian on the basilica and rabbit are
shown in Figures 6.14 and 6.15 and resemble the eigenfunctions of the equilibrium
Laplacian in Figures 6.9 and 6.11, at least near the bottom of the spectrum. The
conformal measures are preserved by the horizontal and vertical reflections, but
there are no longer derived eigenspaces, since the action of P distorts these mea-
sures. In both cases eigenfunction #2 is of H type with reduced support, but
eigenfunction #3 only approximates a doubling of #2 and has full support. It is
symmetric under both reflections. Basilica #4 is of V type, while #11 is of both H
and V types (it is skew-symmetric under both reflections). We also see eigenspaces
of multiplicity two, for example #7 and #8, or #21 and #22, corresponding to
pairs of regions illustrated in Figure 7.1 for which $|z|$ is identical. We never see
multiplicity higher than two because among such corresponding regions there are
never more than two with the same $|z|$ values. On the rabbit we see H types
(#2) and V types (#6), but unfortunately we have not been able to get reliable
accuracy higher up in the spectrum to see the other types of behavior, but these
undoubtedly occur. Already #15 and #16 show puzzling behavior, as they are
neither symmetric nor skew-symmetric with respect to the $z \to -z$ symmetry, yet
they have different eigenvalues so they do not form a multiplicity 2 eigenspace. It
would take higher resolution than we can attain to resolve the ambiguity, and for
this reason we do not attempt to go higher up in the spectrum.

Finally we consider eigenfunctions for the conformal Laplacian on a distorted
basilica (pictures can be found in [Flo08]). This example does not have horizontal
and vertical symmetries (as also is the case for the quasicircle in Figure 6.12). The
first few eigenfunctions appear to be perturbations of the ones in Figure 6.14. We

note that some, like #2, appear to have the same restricted support as H type eigenfunctions. We do not know how to explain this or why there do not appear to be any with the restricted support of V type eigenfunctions. It appears that all eigenspaces have multiplicity 1.

Another striking observation that we are not presently able to explain is the zigzag behavior of the restriction to the central circle of the eigenfunctions of the equilibrium Laplacian. This behavior is more striking for the rabbit than for the basilica, which leads us to speculate that there might be a general statement for all eigenfunctions in the limit as $k \to \infty$. (We also see the same behavior for #2 for the conformal Laplacian.) More generally, it would be interesting to understand the behavior of eigenfunctions of a fixed # and $k \to \infty$. In the case of the Viscek sets discussed in [CSW09], it is possible to answer such questions. Unfortunately, our numerical methods are not adequate to understand even the case $k = 4$.

8. Circles and loops

We single out two types of subsets of $\mathcal{J}$ that we call *circles* and *loops*. Suppose x is a point in $V_m \setminus V_{m-1}$. Then there are k points $x_1, x_2, \ldots, x_k$ in V'_m in increasing order that are identified to obtain x. The portion of $\mathcal{J}$ parameterized by the interval $[x_j, x_{j+1}]$ $(j = 1, \ldots, k-1)$ is called a *loop*. Note that there are $k-1$ loops attached at the point of $\mathcal{J}$ parameterized by x. The *length* of the loops is defined to be $x_{j+1} - x_j = \frac{2^{j-m}}{2^k - 1}$.

The *central circle* is parameterized by the complement (essentially a Cantor set) of the interior of all loops. Note that V'_1 has $2k$ points that divide C into $2k$ intervals. Of these, $2k - 2$ correspond to loops. After we remove these, we are left with the two intervals $[\frac{1}{2(2^k-1)}, \frac{1}{2^k-1}]$ and $[\frac{1}{2} + \frac{1}{2(2^k-1)}, \frac{1}{2} + \frac{1}{2^k-1}]$. The central circle has parameters lying in the union of those intervals. (Note that if $k > 2$ there will be isolated points outside those intervals that are identified with the endpoints, but we do not need to include these in the parametrization.) More generally, a *circle* is parametrized by a Cantor set obtained by all remaining interiors of loops from a pair of intervals $[x, y]$, $[y', x']$, where x, y and y', x' are consecutive but not identified points in V_m and x is identified with x' and y is identified with y'. We define the *length* of the circle to be $2(y - x) = \frac{2}{2^m(2^k-1)}$. It is not hard to see that the circles on $\mathcal{J}$ are indeed topological circles, and any two are either disjoint or intersect at a single point. There are a countable number circles and their union is dense in $\mathcal{J}$, but the union is not all of $\mathcal{J}$, as it has μ-measure zero.

Suppose u is a function defined on the central circle. It is natural to extend u to $\tilde{u}$ on $\mathcal{J}$ by making it constant on all loops, as this clearly minimizes energy. We can easily compute the energy $\mathcal{E}_n(\tilde{u}, \tilde{u})$. It is natural to separate it into two terms corresponding to the initial intervals $I = [\frac{1}{2(2^k-1)}, \frac{1}{2^k-1}]$ and $I' = I + \frac{1}{2}$. Note that I does not subdivide in $V'_2, \ldots, V'_k$, and in V'_{k+1} it splits into the two outer intervals of length $\frac{1}{2^k}|I|$ and $k - 1$ loops that do not contribute to the energy. This process then repeats. Thus the parameter space of the I half of the central circle is exactly a linear Cantor set with dissection ratio $\frac{1}{2^k}$. In V'_{mk+1} we have 2^m intervals of length $\frac{1}{2^{mk}}|I|$, with consecutive endpoints identified in V_{mk+1}. This leads to a new parameterization of half of the central circle $\varphi(s)$ with $s \in [0, 1]$ as follows: map the values $[\frac{l}{2^m}]$ to the points in $\mathcal{J}$ parameterized in order by the points in V_{mk+1} at the endpoints of the intervals. At each step, passing from m to $m + 1$, we insert

one new point in $V_{(m+1)k+1}$ in between each consecutive pair of points in V_{mk+1} from the previous step, so the definition is consistent going from m to $m+1$. This defines $\varphi(s)$ on all dyadic rationals, and we extend it by continuity to $[0,1]$. A similar parameterization works for the other half on $[-1,0]$, and the two join up at the endpoints to give a parametrization of the central circle by a standard circle of circumference 2.

Now we compute for the central circle

$$(8.1) \qquad E_{mk+1}(\tilde{u},\tilde{u}) = 2^{mk+1}(2^k - 1)2^m \sum_{l=-2^m}^{2^m-1} |u(\varphi(\tfrac{l+1}{2^m})) - u(\varphi(\tfrac{l}{2^m}))|^2,$$

so

$$(8.2) \qquad \begin{aligned} \mathcal{E}_{mk+1}(\tilde{u}),\tilde{u} &= 2^{\frac{1}{k}}(2^k - 1)\sum_{l=-2^m}^{2^m-1} |u(\varphi(\tfrac{l+1}{2^m})) - u(\varphi(\tfrac{l}{2^m}))|^2 \\ &= 2^{\frac{1}{k}}(2^k - 1)\tilde{\mathcal{E}}(u \circ \varphi, u \circ \varphi), \end{aligned}$$

where $\tilde{\mathcal{E}}_m$ is the standard dyadic energy on $[0,1]$. Taking the limit as $m \to \infty$ yields

$$(8.3) \qquad \mathcal{E}^{(1)}(\tilde{u},\tilde{u}) = 2^{\frac{1}{k}}(2^k - 1)\tilde{\mathcal{E}}(u \circ \varphi, u \circ \varphi),$$

where $\tilde{\mathcal{E}}$ is the standard energy (H^1 Sobolev space) on the parameter space. Note that $E_{mk+j}(\tilde{u},\tilde{u}) = E_{mk+1}(\tilde{u},\tilde{u})$ for $1 \le j \le k$ because no new points are added to the parametrization of the central circle in the passage from V_{mk+l} to V_{mk+l+1} for $1 \le l \le k-1$. By (3.11)

$$(8.4) \qquad \mathcal{E}_{mk+j}(\tilde{u},\tilde{u}) = 2^{(\frac{1-k}{k})(j-1)}\mathcal{E}_{mk+1}(\tilde{u},\tilde{u}),$$

so

$$(8.5) \qquad \mathcal{E}^{(j)}(\tilde{u},\tilde{u}) = 2^{1-j(\frac{k-1}{k})}(2^k - 1)\mathcal{E}(u \circ \varphi, u \circ \varphi)$$

(here we use $j = k$ rather than $j = 0$ for $\mathcal{E}^{(0)}$). Thus

$$(8.6) \qquad \mathcal{E}(\tilde{u},\tilde{u}) = c_k \mathcal{E}(u \circ \varphi, u \circ \varphi)$$

for

$$(8.7) \qquad c_k = \frac{2(2^k - 1)(1 - 2^{1-k})}{k(2^{1-\frac{1}{k}} - 1)}.$$

More generally, suppose we consider a circle C_n of length $\frac{2}{2^m(2^k-1)}$ that arises in V_m (the central circle has $m = 1$). Again we may parameterize it by $[-1,1]$ and write φ_n for the parametrization map. If u is defined on the circle and $\tilde{u}$ is its harmonic extension, then

$$(8.8) \qquad \mathcal{E}(\tilde{u},\tilde{u}) = 2^{\frac{m-1}{k}}c_k \mathcal{E}(u \circ \varphi_n, u \circ \varphi_n).$$

Let $C_0, C_1, C_2, \ldots$ be the list of all circles in $\mathcal{J}$, with C_0 the central circle, and let $m(n)$ be the value of m assoicated with C_n. The following result was established for $k = 2$ in [RT09]:

Theorem 8.1. *Let u be a continuous function on $\mathcal{J}$. Then $u \in$ dom $\mathcal{E}$ if and only if $u \circ \varphi_n \in$ dom $\tilde{\mathcal{E}}$ for every n and*

$$(8.9) \qquad \mathcal{E}(u,u) = \sum_{n=0}^{\infty} 2^{\frac{m(n)-1}{k}}c_k \tilde{\mathcal{E}}(u \circ \varphi_n, u \circ \varphi_n)$$

is finite.

Proof. Suppose $u \in dom \; \mathcal{E}$. Let $\tilde{u}_N$ denote the harmonic extension of the restriction of u to $C_0 \cup C_1 \cup \ldots \cup C_N$. Then by the previous argument

$$(8.10) \qquad \mathcal{E}(\tilde{u}_N, \tilde{u}_N) = \sum_{n=0}^{N} 2^{\frac{m(n)-1}{k}} c_k \tilde{\mathcal{E}}(u \circ \varphi_n, u \circ \varphi_n).$$

It is routine to show $\mathcal{E}(u, u) = \lim_{N \to \infty} \mathcal{E}(\tilde{u}_N, \tilde{u}_N)$, so (8.9) holds; in particular, the sum is finite and $u \circ \varphi_n \in dom \; \tilde{\mathcal{E}}$ for each n.

Conversely, suppose u is continuous and the sum in (8.9) is finite. Then if we define $\tilde{u}_N$ as above, the previous argument shows that $\tilde{u}_N \in dom \; \mathcal{E}$ and (8.10) holds. Then $\tilde{u}_N$ is a Cauchy sequence in energy and so converges to an element in $dom \; \mathcal{E}$ that we may identify with u. $\qquad \square$

There is a close relationship between the set of circles and the supports of the derived vertical eigenspaces as described in the proof of Theorem 7.3. Each of the regions contains a circle and some loops attached to it (see Figures 7.2 and 7.4). Each circle occurs infinitely often, with fewer attached loops as the order of the derived eigenvalue increases.

We note that $P^{(k)}$ maps C_0 to C_0 in a two-to-one fashion and is conjugate $(\varphi_0^{-1} P^{(k)} \varphi_0)$ to the doubling map on the parameter circle. Since the doubling map multiplies the standard energy $\tilde{\mathcal{E}}$ by 4, it follows that the contribution from C_0 to the total energy is also multiplied by 4:

$$(8.11) \qquad c_k \tilde{\mathcal{E}}(u \circ P^{(k)} \circ \varphi_0, u \circ P^{(k)} \circ \varphi_0) = 4 c_k \tilde{\mathcal{E}}(u \circ \varphi_0, u \circ \varphi_0).$$

One can also derive (8.11) directly from the definition. Although (8.11) appears to conflict with (3.26), it has to be noted that the inverse image of C_0 under $P^{(k)}$ is much larger than C_0, and the entire inverse image contributes to the left side of (3.24). In passing from the global energy identity to the local one the value is reduced by a factor of $\frac{1}{2^{k}-1}$, so the factor 2^{k+1} in (3.24) becomes 4 in (8.11). There are similar but more complicated identities relating to the transformation of energies on other circles under the iteration of P.

It is useful to decompose the sum in (8.9) into the contributions from circles with $m(n)$ in a given residue class modulo k. So we define

$$(8.12) \quad \tilde{\mathcal{E}}^{(j)}(u, u) = \sum_{m(n) \equiv j(k)} 2^{\frac{m(n)}{k}} (2^k - 1) \tilde{\mathcal{E}}(u \circ \varphi_n, u \circ \varphi_n) \text{ for } j = 0, 1, \ldots, k - 1.$$

Now suppose we fix a circle C_n with $m(n) \equiv j(k)$ and let $\tilde{u}_n$ be the harmonic extension of $u|_{C_n}$. The analogs of (8.1), (8,2), and (8.3) are

$$(8.13)$$

$$E_{m(n)+mk}(\tilde{u}_n, \tilde{u}_n) = 2^{m(n)+mk}(2^k - 1) \sum_{l=-2^m}^{2^m - 1} |u(\varphi_n(\frac{l+1}{2^m})) - u(\varphi_n(\frac{l}{2^m}))|^2,$$

$$(8.14) \qquad \mathcal{E}_{m(n)+mk}(\tilde{u}_n, \tilde{u}_n) = 2^{\frac{m(n)}{k}}(2^k - 1)\tilde{\mathcal{E}}_m(u \circ \varphi_n, u \circ \varphi_n)$$

and

$$(8.15) \qquad \mathcal{E}^{(j)}(\tilde{u}_n, \tilde{u}_n) = 2^{\frac{m(n)}{k}}(2^k - 1)\tilde{\mathcal{E}}_m(u \circ \varphi_n, u \circ \varphi_n).$$

There will be no new subdivision points in C_n when we pass from $m(n) + mk$ to $m(n) + mk + p$ for $p \leq k - 1$, so

$$(8.16) \qquad E_{m(n)+mk+p}(\tilde{u}_n, \tilde{u}_n) = E_{m(n)+mk+p}(\tilde{u}, \tilde{u})$$

so

(8.17) $\quad \mathcal{E}^{(j+p)}(\tilde{u}_n, \tilde{u}_n) = 2^{\frac{m(n)+(1-k)p}{k}}(2^k - 1)\tilde{\mathcal{E}}(u \circ \varphi_n, u \circ \varphi_n)$ for $0 \le p \le k - 1$.

If we sum over all circles and sort according to residue classes of $m(n)$, we obtain, for $0 \le q \le k - 1$,

(8.18) $$\mathcal{E}^{(q)}(u, u) = \sum_{j=0}^{k-1} 2^{(\frac{1-k}{k})[q-j]}\tilde{\mathcal{E}}^{(j)}(u, u),$$

where we interpret $[q - j]$ as $q - j$ if $j \le q$ and $k + q - j$ if $j > q$. Note that for each fixed j the values of $[q - j]$ cycle through the integers $0, 1, \ldots, k - 1$. By averaging (8.18) over q we recover (8.9).

We also note that, although each circle has μ-measure zero, we can express the integral of continuous function in terms of the ordinary integrals of its restrictions to all the circles as a limit of sums. Suppose we fix a circle C_n with $m(n) = m$. The length of the circle is $\frac{2}{2^m(2^k-1)}$, and there are two intervals of half this length in $C \setminus V_m$ that parameterize C_n and all the loops to which they attach. We may approximate the integral over these intervals by

(8.19) $$\frac{1}{2^m(2^k - 1)} \int_{-1}^{1} f(\varphi_n(t))dt.$$

The same approximation is valid for $C \setminus V_{m+j}$ for $j \le k$, but in $C \setminus V_{m+k}$ the intervals subdivide and only two intervals of length $\frac{2}{2^{m+k}(2^k-1)}$ parameterize C_n and some of the loops that attach to it. In general, in $C \setminus V_j$ with $j \ge m$, the intervals representing C_n will be subdivided $l = [\frac{j-m}{k}]$ times, and each time the total length is reduced by a factor of $\frac{1}{2^k-1}$. Thus

(8.20) $$\sum_{m(n) \le j} \frac{1}{2^{m(n)+[\frac{j-m(n)}{k}](k-1)}(2^k - 1)} \int_{-1}^{1} f(\varphi_n(t))dt$$

is the approximation at level j. It is easy to see that (8.20) converges to $\int_{\mathcal{J}} f d\mu$ as $j \to \infty$.

9. Eigenfunctions on loops and circles

Consider a loop $\mathcal{L}$ of length $\frac{2^{j-m}}{2^k-1}$. We regard the point z_0 where the loops join the rest of $\mathcal{J}$ as the *boundary* point. In the parameter space z_0 corresponds to the two boundary points of the interval $I(\mathcal{L})$ that parameterizes $\mathcal{L}$. Everything else is *interior*. It makes sense to consider the eigenvalue equation on $\mathcal{L}$:

(9.1) $$-\Delta_\mu u = \lambda u \ \ on \ \ \mathcal{L} \setminus z_0,$$

(9.2) $$u(z_0) = a.$$

If there exists a nonzero solution with $a = 0$, we say that λ is a *Dirichlet eigenvalue* on $\mathcal{L}$. The set of Dirichlet eigenvalues forms a sequence

(9.3) $$0 < \lambda_1(\mathcal{L}) \le \lambda_2(\mathcal{L}) \le \ldots \to \infty.$$

Let $\lambda_n = \lambda_n(\mathcal{L})$, where $\mathcal{L}$ is a loop of the largest length $(m = 1, j = 1)\frac{1}{2^k-1}$. Then for a general loop we have from (4.8) that

(9.4) $$\lambda_n(\mathcal{L}) = 2^{(1+\frac{1}{k})(m-j)}\lambda_n,$$

and the associated eigenfunctions are mapped to each other by appropriate iterations of P. We may regard these as similarities (they are similarities on the parameter space). Note that for any positive fixed λ, $\lambda_1(\mathcal{L}) > \lambda$ for all sufficiently small loops (equivalently, all but a finite number of loops), and this implies that λ is not a Dirichlet eigenvalue for such loops.

It is easy to see that (9.1) has a unique solution for any λ that is not a Dirichlet eigenvalue. In particular, if $a = 0$, then $u \equiv 0$. Let u_λ denote the unique solution for $a = 1$ when $\mathcal{L}$ is a loop of largest length $\frac{1}{2^k - 1}$. Then the solution to the eigenvalue equation (9.1) on a general loop must have the form

$$(9.5) \qquad u(z_0) u_{2^{(1+\frac{1}{k})(j-m)}\lambda} \circ S_{\mathcal{L}}$$

provided $\lambda \neq 2^{(1+\frac{1}{k})(j-m)}\lambda_n$ for any n, where $S_{\mathcal{L}}$ denotes the similarity mapping of the small loop to the large loop.

Now suppose u is a global λ-eigenfunction on $\mathcal{J}$. Then for any sufficiently small loop, u has the form (9.5).

Theorem 9.1. *Let u be a global eigenfunction of Δ_μ on $\mathcal{J}$, and suppose u is even or odd with respect to R_H and R_V. Then there are loops on which u vanishes identically.*

Proof. It suffices to prove this for primitive eigenfunctions, in which case u has either $+-$ or $-+$ symmetry. Hence it is odd with respect to either R_H or R_V. Thus u vanishes on the fixed points of R_H or R_V, and there are infinitely many of these. If we choose a sufficiently small loop having one of these fixed points as boundary point z_0, then $u(z_0) = 0$ and (9.5) shows that u vanishes on the loop. $\square$

Conjecture 9.2. *The same conclusion holds for all eigenfunctions.*

The only way this can fail is for an eigenspace of nontrival multiplicity when u is a linear combination of H and V primitive eigenfunctions. This happens on the basilica for a primitive eigenvalue in numbers 212 and 213, yet the two eigenfunctions have loops where they both vanish. It also happens all the time for derived eigenvalues, but in all the examples the primitive eigenfunctions are locally equivalent to derived eigenfunctions.

Next we consider the restrictions of global eigenfunctions to circles. For simplicity we just consider the central circle C_0. In order to proceed we need to make the following assumptions on the eigenvalue λ:

$$(9.6) \qquad \lambda \neq 2^{(1+\frac{1}{k})(m-j)}\lambda_n$$

for any n and any m and $j \leq k - 1$. This makes (9.5) valid on any loop. Since $\mathcal{J}$ is the union of C_0 and all loops that attach to it, it follows that any λ-eigenfunction is uniquely determined by its restriction to C_0. (Of course there are eigenfunctions which vanish on C_0, so (9.6) does not always hold.) It should be possible to express the eigenvalue equation entirely in terms of the values of u on points in C_0. We will indicate, at least in principle, how this can be done.

The points in $V_{mk+1} \cap C_0$ are paramterized by $\varphi(\frac{l}{2^m})$ for $0 \leq l < 2^m$. Then $V_{mk+j} \cap C_0 = V_{mk+1} \cap C_0$ for $j = 1, \ldots, k$. In other words, no new points in C_0 are created in the next $k - 1$ subdivisions, because the intervals in the external ray parametrization between consecutive points in C_0 are the smallest intervals in V'_m. For a fixed value of l, the neighbors of $x = \varphi(\frac{1}{2^m})$ in $V_{mk+j} \cap C_0$ are exactly $\varphi(\frac{l-1}{2^m})$ and $\varphi(\frac{l+1}{2^m})$. Of course x will have $2k - 2$ neighbors in each of the graphs

Γ_{mk+j} that lie on the loops that attach at x, and these neighbors will vary with j. For each loop there will be exactly four such neighbors. In Γ_m we denote the neighbors $y_1, \ldots, y_{k-1}$ and $z_1, \ldots, z_{k-1}$, where y_j and z_j lie on the same loop and have distance $\frac{1}{(2^k-1)2^{mk+j}}$ from x in the external ray parametrization. These (y_j and z_j) are also neighbors in $\Gamma_{mk+2}, \Gamma_{mk+3}, \ldots, \Gamma_{mk+j}$, but in Γ_{mk+j+1} their intervals get subdivided and we obtain new neighbors y_j' and z_j' in the same loop at distance $\frac{1}{(2^k-1)2^{(m+1)k+j}}$ to x. These remain neighbors in Γ_{mk+l} for $j < l \le k$.

Recall that we are using the discrete energy $\frac{1}{k}(\mathcal{E}_{mk+1}(u,v) + \mathcal{E}_{mk+2}(u,v) + \ldots + \mathcal{E}_{(m+1)k}(u,v))$ to approximate $\mathcal{E}(u,v)$, and the weight assigned to each point in $V_{(m+1)k}$ to approximate μ is $2^{-(m+1)k}$. Thus the approximate Laplacian $\Delta_{(m+1)k}$ is given by

$$(9.7) \qquad -\Delta_{(m+1)k}u(x) = 2^{(m+1)k}\frac{1}{k}\sum_{j=1}^{k}2^{(\frac{1-k}{k})(mk+j)}E_{mk+j}(u,v),$$

where v is defined on $V_{(m+1)k}$ by $v(y) = \delta_{xy}$. Now

$$(9.8) \qquad \begin{aligned} E_{mk+1}(u,v) = (2^k-1)2^{mk+1}[(2u(x) - u(\varphi(\tfrac{l+1}{2^m})) - u(\varphi(\tfrac{l-1}{2^m}))) \\ + \sum_{p=1}^{k-1}2^{-p}(2u(x) - u(y_p) - u(z_p))], \end{aligned}$$

and in general, for $1 \le q \le k$,

$$(9.9) \qquad \begin{aligned} E_{mk+j}(u,v) = (2^k-1)2^{mk+1}[2u(x) - u(\varphi(\frac{l+1}{2^m})) - u(\varphi(\frac{l-1}{2^m})) \\ + \sum_{p=1}^{k-j}2^{-p}(2(u(x) - u(y_p) - u(z_p))) \\ + \sum_{p=k-j+1}^{k-1}2^{k-p}(2(u(x) - u(y_p') - u(z_p')))]. \end{aligned}$$

Substituting (9.9) into (9.7) and collecting terms we obtain

$$(9.10)$$
$$\begin{aligned} -\Delta_{(m+1)k}u(x) \\ = 2^{(m+1)k+1}(2^k-1)\frac{1}{k}[(\sum_{j=1}^{k}2^{j(\frac{1+k}{k})})(2u(x) - u(\varphi(\frac{l+1}{2^m})) - u(\varphi(\frac{l-1}{2^m}))) \\ + \sum_{p=1}^{k-1}2^{-p}(\sum_{j=1}^{k-p}2^{j(\frac{1-k}{k})})(2u(x) - u(y_p) - u(z_p)) \\ + \sum_{p=1}^{k-1}2^{k-p}(\sum_{k-p+1}^{k}2^{j(\frac{1-k}{k})})(2u(x) - u(y_p') - u(z_p'))]. \end{aligned}$$

This, of course, can be simplified. But the key point is that if u is a λ-eigenfunction where λ satisfies the assumption (9.6), we can use (9.5) to express all the terms $u(y_p), u(z_p), u(y_p')$, and $u(z_p')$ as multiples of $u(x)$. Thus

$$(9.11) \qquad\qquad\qquad -\Delta_{(m+1)k}u \approx \lambda u$$

may be written as

$$(9.12) \quad 2^{(m+1)k} A_k (2u(x) - u(\varphi(\frac{l+1}{2^m})) - u(\varphi(\frac{l-1}{2^m}))) \approx (\lambda + B_k(x, m, \lambda))u(x)$$

for constants A_k and B_k. Note that B_k depends on x because the lengths of the loops that attach to x vary. More precisely, it depends only on the level where x first appears. B_k also depends on λ via (9.5), and this is a nonlinear dependence. Of course (9.12) is only approximately true, and what we are interested in is the limit as $m \to \infty$. We expect that the limit will be an eigenvalue equation (the eigenvalue will depend on λ in a nonlinear fashion) for $u \circ \varphi$ for a Laplacian built from the standard energy and some new measure that also depends on λ.

A simple special case is that of $\lambda = 0$, or harmonic functions. While there are no global harmonic functions on $\mathcal{J}$, there are piecewise harmonic functions that enable us to describe the Green's function. Let us fix two points z_0, z_1 in $\mathcal{J}$, and to begin we will assume that both are points on the same circle C_n of length L_n, $z_0 = \varphi_n(t_0)$, $z_1 = \varphi_n(t_1)$. We construct a function $G(t)$ on the parameter circle so that $-G'' = \delta_{t_1} - \delta_{t_0}$. This only determines G up to an additive constant, so we adjoin the arbitrary condition $G(t_0) = 0$. It is easy to see that

$$(9.13) \qquad G(t) = \begin{cases} \frac{1}{L_n}(t - t_0)(L_n - t_1 + t_0) & \text{if} \quad t_0 \le t \le t, \\ \frac{1}{L_n}(L_n - t + t_0)(t_1 - t_0) & \text{if} \quad t_1 \le t \le L_n + t_0 \end{cases}$$

(here G is extended to be periodic of period L_n). Note that $G(t_0) = G(L_n + t_0) = 0$ and both expressions give $G(t_1) = \frac{(t_1 - t_0)(L_n - t_1 + t_0)}{L_n}$, so G is a piecewise linear and continuous, and the jumps in G' yield $-G'' = \delta_{t_1} - \delta_{t_0}$.

Next we transfer G to $\mathcal{J}$ by defining

$$(9.14) \qquad\qquad\qquad \tilde{G}(\varphi_n(t)) = G(t)$$

and making $\tilde{G}$ constant on all loops that attach to C_n. We may give a more explicit description of $\tilde{G}$ in terms of the external ray parametrization. The circle C_n is parameterized by a pair of Cantor sets whose extremities are identified, together with some discrete points (when $k \ge 3$) identified with some points on the Cantor set. Call this set C_n'. The complement of C_n' in the external ray parameter circle is a countable union of intervals $\cup I_j$, where the endpoint a_j, b_j of each I_j are identified. Of course the interval I_j parametrizes the interior of a loop that attaches at the endpoints, so

$$(9.15) \qquad\qquad \tilde{G}(x) = \tilde{G}(a_j) \text{ for } x \in I_j, \quad a_j \in C_j.$$

Note that (9.14) and (9.15) together define $\tilde{G}$ on $\mathcal{J}$. To show the dependence on z_0, z_1 and n we write $\tilde{G}_n(z_0, z_1)(x)$.

Because $\tilde{G}$ is constant on loops, only the first term in (9.10) is nonzero, so

$$(9.16) \qquad -\Delta_{(m+1)k} \tilde{G}_0(z_0, z_1)(x) = B_k 2^{mk} (2G(\frac{l}{2^m}) - G(\frac{l+1}{2^m}) - G(\frac{l-1}{2^m}))$$

if $x = \varphi_0(\frac{l}{2^m})$, and $-\Delta_{(m+1)k} \tilde{G}_0(z_0, z_1)$ vanishes outside C_0. Thus

$$(9.17) \qquad\qquad\qquad -\Delta_\mu \tilde{G}_0(z_0, z_1) = B_k(\delta_{z_1} - \delta_{z_0}).$$

A similar expression holds for any circle C_n.

We may now construct a Green's function $G_z(x)$ for any point $z \in \mathcal{J}$ that satisfies

(9.18) $$-\Delta_\mu G_z = \delta_z - \delta_{z_0} \text{ and } G_z(z_0) = 0$$

where $z_0 = \varphi_0(0)$ is a fixed base point. For simplicity we first describe the case where z belongs to a circle. Then there is a unique chain of circles $C_0, C_{n_1}, C_{n_2}, \ldots,$ C_{n_N} and points $z_0, z_1, \ldots, z_N = z$ such that z_j and z_{j+1} both belong to C_j (this means $z_j = C_{j-1} \cap C_j$ for $0 < j < N$). It is easy to see that

(9.19) $$G_z = \frac{1}{B_k}(\tilde{G}_0(z_0, z_1) + \sum_{j=1}^{N}(\tilde{G}_{n_j}(z_j, z_{j+1}) - \tilde{G}_{n_j}(z_j, z_{j+1})(z_0)))$$

satisfies (9.18). If z does not belong to a circle, then there is a unique infinite chain of circles and points such that $z_n \to z$ as $N \to \infty$, and then (9.19) holds with $N = \infty$. Note that G_z is a piecewise linear function on circles.

We can use the Green's function to "invert" the Laplacian as follows. Since the Laplacian is neither one-to-one nor onto, we impose the condition

(9.20) $$\int_{\mathcal{J}} f(y) d\mu(y) = 0$$

on the right side of

(9.21) $$-\Delta_\mu u = f$$

to assure existence, and we assume

(9.22) $$u(z_0) = 0$$

to determine a unique solution. The solution is then given by integration against G_z,

(9.23) $$u(x) = \int_{\mathcal{J}} G_y(x) f(y) d\mu(y).$$

Indeed,

(9.23) $$\begin{aligned} -\Delta_\mu u(x) &= \int_{\mathcal{J}}(\delta_y(x) - \delta_{z_0}(x)) f(y) d\mu(y) \\ &= f(x) - (\int_{\mathcal{J}} f(y) d\mu(y)) \delta_{z_0}(x) \\ &= f(x) \end{aligned}$$

by (9.18) and (9.20), and $u(z_0) = 0$ by (9.18).

We can also solve

(9.21') $$-\Delta_{\mu'} u = f$$

and (9.22) under the assumption

(9.20') $$\int_{\mathcal{J}} f(y) d\mu'(y)$$

by

(9.23') $$u(x) = \int_{\mathcal{J}} G_y(x) f(y) d\mu'(y)$$

for any finite Borel measure on $\mathcal{J}$ that assigns positive measure to open sets.

Acknowledgements

The authors would like to thank Jun Kigami, John H. Hubbard, Luke Rogers, and John Smillie for many helpful conversations.

References

[ADS10] Tarik Aougab, Chu Yue (Stella) Dong, and Robert S. Strichartz, *Laplacians of a family of quadratic julia sets II*, Comm. Pure Appl. Math., to appear.

[ASST03] Bryant Adams, S. Alex Smith, Robert S. Strichartz, and Alexander Teplyaev, *The spectrum of the Laplacian on the pentagasket*, Fractals in Graz 2001, Trends Math., Birkhäuser, Basel, 2003, pp. 1–24. MR2091699 (2006g:28017)

[Bar98] Martin T. Barlow, *Diffusions on fractals*, Lectures on probability theory and statistics (Saint-Flour, 1995), Lecture Notes in Math., vol. 1690, Springer, Berlin, 1998, pp. 1–121. MR1668115 (2000a:60148)

[Bra89] Bodil Branner, *The Mandelbrot set*, Chaos and fractals (Providence, RI, 1988), Proc. Sympos. Appl. Math., vol. 39, Amer. Math. Soc., Providence, RI, 1989, pp. 75–105. MR1010237

[CSW09] Sarah Constantin, Robert S. Strichartz, and Miles Wheeler, *Analysis of the Laplacian and spectral operators on the Vicsek set*, Comm. Pure Appl. Anal. **10** (2011), no. 1, 1–44. MR2746525

[DH84] Adrien Douady and John H. Hubbard, *Etude dynamique des polynomes complexes i*, Publ. Math. d'Orsay (1984).

[Flo08] Taryn C. Flock, *Laplacians on a family of quadratic julia sets*, `http://www.math.cornell.edu/~taryn/data.html`, September 2008.

[FS92] M. Fukushima and T. Shima, *On a spectral analysis for the Sierpiński gasket*, Potential Anal. **1** (1992), no. 1, 1–35. MR1245223 (95b:31009)

[Kig01] Jun Kigami, *Analysis on fractals*, Cambridge Tracts in Mathematics, vol. 143, Cambridge University Press, Cambridge, 2001. MR1840042 (2002c:28015)

[KL93] Jun Kigami and Michel L. Lapidus, *Weyl's problem for the spectral distribution of Laplacians on p.c.f. self-similar fractals*, Comm. Math. Phys. **158** (1993), no. 1, 93–125. MR1243717 (94m:58225)

[RT09] Luke G. Rogers and Alexander Teplyaev, *Laplacians on the Basilica julia sets*, Comm. Pure Appl. Anal. **9** (2010), no. 1, 211–231. MR2556753 (2011c:28024)

[Str06] Robert S. Strichartz, *Differential equations on fractals*, Princeton University Press, Princeton, NJ, 2006, A tutorial. MR2246975 (2007f:35003)

[Zho09] Denglin Zhou, *Spectral analysis of laplacians on viscek sets*, Pac. J. Math. **241** (2009), 369–398.

[Zho10] _____ , *Criteria for spectral gaps of Laplacians on fractals*, J. Fourier Anal. Appl. **16** (2010), no. 1, 76–96. MR2587582 (2011b:28026)

Department of Mathematics, University of California Berkeley, Berkeley, California 94709

E-mail address: `tflock@math.berkeley.edu`

Department of Mathematics, Malott Hall, Cornell University, Ithaca, New York 14853

E-mail address: `str@math.cornell.edu`